PHYSICS OF FLUIDS 17, 035101 (2005)

Modeling return to isotropy using kinetic equations

Blair Perot[a)] and Chris Chartrand
Department of Mechanical Engineering, University of Massachusetts, Amherst, Massachusetts 01003

(Received 7 July 2004; accepted 27 October 2004; published online 28 January 2005)

Kinetic equations modeling the behavior of the velocity probability density function (PDF) in homogeneous anisotropic decaying turbulence are hypothesized and their implications for return-to-isotropy are investigated. Anisotropic turbulent decay is a parametrically simple but theoretically complex turbulent flow that is dominated by nonlinear interactions. The physical implications of the Bhatnagar–Gross–Krook model, a relaxation model, and the Fokker–Planck model for the "collision" term in the PDF evolution equation are analyzed in detail. Using fairly general assumptions about the physics, three different parameter-free return-to-isotropy models are proposed. These models are compared with experimental data, classical models, and analytical limits. The final model expression is particularly interesting, and can easily be implemented in classic Reynolds stress transport models.
[DOI: 10.1063/1.1839153]

I. INTRODUCTION

In most turbulent flows of interest the turbulent velocity fluctuations are anisotropic, that is, they differ in magnitude depending on their orientation. One aspect of Reynolds stress transport models (and other more advanced models) that distinguishes them from simple two-equation transport models like k-ε is their ability to more accurately model turbulence anisotropy. The degree of anisotropy is important because it can directly impact how turbulence affects the mean flow.

In the absence of any driving mechanism, anisotropic turbulent flows tend to return to an isotropic state (the state of least order). This nonlinear process is often called return-to-isotropy. It was identified early on in the development of Reynolds stress transport models and first modeled by Rotta.[1] Since that time, the return-to-isotropy process has been extensively investigated and modeled.[2–11]

The return-to-isotropy problem is of significant theoretical interest in the theory of turbulence because it is entirely due to nonlinear interactions. In theory (if the Navier–Stokes equations are solved), the return process is reversible. However, averaging processes (such as the ensemble averages used in RANS models) lead to irreversibility. A similar effect happens in thermodynamics—molecular collisions are completely reversible, but their thermodynamic average behavior is not. This means that at the RANS modeling level, return to isotropy is an irreversible process and should be modeled as such. Existing models for return-to-isotropy tend to make extensive use of mathematical concepts, such as the Cayley–Hamilton theorem, realizability, Taylor series expansions, and fixed-point analysis. The resulting models invariably have at least one model "constant" that must be set via experiments.

In this work, we are interested in deriving models for the return process (or setting the unknown constants in existing models) based on physical ideas as well as mathematical tools. We make the assumption that turbulence behaves as a kinetic process, and that kinetic models of turbulence may lead to some useful insights about the return process. The advantage of this approach is that by assuming some very general physical conditions, the resulting models can be made to be free of any tunable model constants.

In Sec. II, the classic Reynolds stress transport equation approach to modeling return-to-isotropy is briefly reviewed. We use these classic results as a reference since this is the approach that is most widely understood by most readers. In Sec. III we consider return-to-isotropy from the perspective of the Bhatnagar–Gross–Krook (BGK)[12] approximation to the Boltzmann equation. Classic linear return models result from this kinetic equation. The deficiencies of the BGK approach are largely solved by two parameter-free relaxation collision models developed and tested in Sec. IV. Section V investigates the predictive performance of these models for five different experimental cases. The relaxation model is extended in Sec. VI to enable any desired Reynolds stress return behavior, and another parameter-free model is proposed that has some unique properties and better agreement with experimental data. Section VII explores the implications and connections to the Fokker–Planck collision model, and the results are discussed in Sec. VIII, where some speculation is presented as to what these kinetic models imply about turbulent eddy interactions.

II. REYNOLDS STRESS TRANSPORT MODELS

In the absence of any mean flow the evolution of the Reynolds stress tensor R_{ij} in homogeneous but anisotropic turbulence evolves according to the equation

$$\frac{\partial R_{ij}}{\partial t} = -2\upsilon\overline{u'_{i,k}u'_{j,k}} + \overline{p(u'_{i,j}+u'_{j,i})}. \tag{1}$$

The first term on the right-hand side is the dissipation rate tensor and the second term is the slow pressure strain. The pressure strain is considered "slow" in this situation because

[a)]Electronic mail: perot@ecs.umass.edu

the pressure in this term depends only on the turbulence not on the "rapid" mean flow velocity gradients (since there are none in this situation). Both terms require modeling. However, one half the trace of the dissipation tensor is the dissipation rate, $\varepsilon = \upsilon u'_{i,k} u'_{j,k}$, which is assumed to be known (given by another transport equation model), and the trace of the pressure-strain term is zero in incompressible flows.

The most common modeling approach is to assume that the dissipation tensor is close to isotropic. If small anisotropy in the dissipation tensor exists then it is included with the pressure strain model. The slow pressure strain and anisotropic dissipation are then collectively modeled as a "return-to-isotropy" term. There are reasons to suggest that modeling dissipation anisotropy and slow pressure strain separately is also advantageous,[13,14] but for simplicity we retain the "collective" approach described above. The simplest model (due to Rotta) is that the return-to-isotropy term is proportional to the Reynolds stress anisotropy. This gives a Reynolds stress transport model of the form

$$\frac{\partial R_{ij}}{\partial t} = -\frac{2}{3}\varepsilon\delta_{ij} - \hat{C}_R \varepsilon\left(\frac{R_{ij}}{K} - \frac{2}{3}\delta_{ij}\right). \tag{2}$$

The return-to-isotropy term will tend to drive the Reynolds stress tensor towards an isotropic state as time proceeds. The rate at which this happens is governed by the Rotta constant $\hat{C}_R$. This return model is the simplest possible one, and is linear in the Reynolds stress anisotropy, $a_{ij} = \left[(R_{ij}/K) - \frac{2}{3}\delta_{ij}\right]$. Equation (2) appears to imply return-to-isotropy for any positive value of $\hat{C}_R$. In fact this is not the case, $\hat{C}_R$ must be greater than 1. To see this we look at the evolution equation for R_{ij}/K which should tend towards $\frac{2}{3}\delta_{ij}$,

$$\frac{\partial (R_{ij}/K)}{\partial t} = \frac{1}{K}\frac{\partial R_{ij}}{\partial t} - \frac{R_{ij}}{K^2}\frac{\partial K}{\partial t} = -(\hat{C}_R - 1)\frac{\varepsilon}{K}\left(\frac{R_{ij}}{K} - \frac{2}{3}\delta_{ij}\right). \tag{3}$$

The isotropic dissipation actually causes the Reynolds stress tensor to move away from isotropy which must be counteracted by the return term. $\hat{C}_R$ is actually a parameter, not a strict constant, which can be (and often is) a function of the Reynolds stress invariants and turbulent Reynolds number. Due to the strict requirement described above the splitting $\hat{C}_R = 1 + C_R$ is useful. This gives a model equation of the form

$$\frac{\partial R_{ij}}{\partial t} = -\varepsilon\frac{R_{ij}}{K} - C_R\varepsilon\left(\frac{R_{ij}}{K} - \frac{2}{3}\delta_{ij}\right), \tag{4}$$

where $C_R > 0$. Typical values for C_R lie between 0.5 and 1.0 (Durbin).[15] Launder, Reece, and Rodi[16] suggest a value of 0.8. No return to isotropy is the case of $C_R = 0$. Physically, the no-return limit appears to occur at low Reynolds numbers. In addition, the no-return limit is often enforced in the two-component limit (where one of the Reynolds stress diagonals goes to zero faster than the others, such as near walls). For this reason C_R is often not a constant but is actually a parameter that depends on the turbulent Reynolds number and Reynolds stress invariants.[7,17]

It is helpful to propose a general model for the Reynolds stress evolution,

$$\frac{\partial R_{ij}}{\partial t} = -\frac{\varepsilon}{2K}\left(\Pi_{im}R_{mj} + \Pi_{jm}R_{mi}\right), \tag{5}$$

where the dimensionless Π_{ij} is some as yet unspecified model. Expanding this model as $\Pi_{ij} = \delta_{ij} + \hat{\Pi}_{ij}$ gives

$$\frac{\partial R_{ij}}{\partial t} = -\frac{\varepsilon}{K}R_{ij} - \frac{\varepsilon}{2K}\left(\hat{\Pi}_{im}R_{mj} + \hat{\Pi}_{jm}R_{mi}\right), \tag{6}$$

so it is clear that $\hat{\Pi}_{ij}$ is the return part of the model. The trace of the last term should be zero, so we have a single constraint on the model, $\hat{\Pi}_{ij}R_{ji} = 0$. It is not necessary that $\hat{\Pi}_{ij}$ be symmetric. The explicit inclusion of the Reynolds stress in Eq. (5) means that this general model can be strongly realizable (Schumann,[18] Lumley[2]) if $\hat{\Pi}_{ij}$ is finite. If one component of the turbulence goes to zero then this model will also make the time derivative of that component go to zero. However, in the unusual circumstance that $\hat{\Pi}_{ij}$ becomes singular (goes to infinity) this model can potentially violate strong realizability. The classic linear return model described above is given by $\hat{\Pi}_{ij} = C_R\left(\delta_{ij} - \frac{2}{3}KR_{ij}^{-1}\right)$. This model becomes singular in the two-component limit (because of the Reynolds stress inverse). The classic linear model satisfies weak realizability[19] if $C_R > 0$, but for the linear model to satisfy strong realizability C_R must go to zero in the two-component limit.

Slightly more complex nonlinear models for return-to-isotropy have the general form

$$\frac{K}{\varepsilon}\frac{\partial a_{ij}}{\partial t} = -C_R(a_{ij}) + C_N\left(a_{ik}a_{kj} - a_{nk}a_{kn}\frac{\delta_{ij}}{3}\right). \tag{7}$$

Cubic and higher order nonlinear models can also be represented by this quadratically nonlinear model due to the Cayley-Hamilton theorem. Sarkar and Speziale[4] suggest values of $C_R = 0.7$ and $C_N = 1.05$.

The realizability conditions are clearer when this model is written in terms of the Reynolds stresses,

$$\frac{\partial R_{ij}}{\partial t} = -\frac{\varepsilon}{K}R_{ij} - \left\{C_R - C_N\left[\frac{R_{nk}R_{kn}}{2K^2} - \frac{4}{3}\right]\right\} \times \frac{\varepsilon}{K}\left(R_{ij} - \frac{2}{3}K\delta_{ij}\right) + C_N\frac{\varepsilon}{K^2}\left(R_{ik}R_{kj} - \frac{R_{nk}R_{kn}}{2K}R_{ij}\right). \tag{8}$$

Pre- and postmultiplying this expression by the eigenvector matrix $\mathbf{Q}$ diagonalizes the Reynolds stress tensor ($\mathbf{Q}^T\mathbf{R}\mathbf{Q} = \mathbf{D}$), so

$$\mathbf{Q}^T\frac{\partial \mathbf{R}}{\partial t}\mathbf{Q} = -\frac{\varepsilon}{K}\mathbf{D} - \left\{C_R - C_N\left[\frac{R_{nk}R_{kn}}{2K^2} - \frac{4}{3}\right]\right\} \times \frac{\varepsilon}{K}\left(\mathbf{D} - \frac{2}{3}K\mathbf{I}\right) + C_N\frac{\varepsilon}{K^2}\left(\mathbf{D}\mathbf{D} - \frac{R_{nk}R_{kn}}{2K}\mathbf{D}\right), \tag{9}$$

since

$$\mathbf{Q}^T \frac{\partial \mathbf{R}}{\partial t}\mathbf{Q} = \frac{\partial \mathbf{D}}{\partial t} + \mathbf{D}\left(\frac{\partial \mathbf{Q}^T}{\partial t}\mathbf{Q}\right) - \left(\frac{\partial \mathbf{Q}^T}{\partial t}\mathbf{Q}\right)\mathbf{D}$$

the off diagonal evolution is trivial, and the diagonal components individually satisfy the right-hand side of Eq. (9). Weak realizability is satisfied as long as $C_R - C_N[(R_{nk}R_{kn}/2K^2) - \frac{4}{3}] \geq 0$. Strong realizability requires equality on this previous expression and $1 + C_N[R_{nk}R_{kn}/2K^2] \geq 0$. The quantity $R_{nk}R_{kn}/2K^2$ appears frequently and is related to the second invariant of the anisotropy tensor via $R_{nk}R_{kn}/2K^2 = \frac{2}{3} + \frac{1}{2}a_{nk}a_{kn}$.

The model expression for the nonlinear return model is

$$\Pi_{ij} = \delta_{ij} + \left\{ C_R - C_N\left[\frac{R_{nk}R_{kn}}{2K^2} - \frac{4}{3}\right]\right\}\left(\delta_{ij} - \frac{2}{3}KR^{-1}_{ij}\right) - C_N\left(\frac{R_{ij}}{K} - \frac{R_{nk}R_{kn}}{2K^2}\delta_{ij}\right). \tag{10}$$

The singularity due to R^{-1}_{ij} is weakly realizable as long as the leading coefficient is positive. It is strongly realizable if this leading coefficient is zero in the two-component limit and the coefficient of δ_{ij} is positive.

III. BHATNAGAR–GROSS–KROOK COLLISION MODELS

In homogeneous turbulence in the absence of mean accelerations or mean pressure gradients the evolution equation for the velocity probability density function (PDF) is

$$\frac{\partial f}{\partial t} = \left.\frac{df}{dt}\right|_{collisions}. \tag{11}$$

This equation governs the decay of anisotropic homogeneous turbulence, which is the focus of this work. One of the simplest collision models is a relaxation of the PDF to some known equilibrium form

$$\frac{\partial f}{\partial t} = -\frac{\varepsilon}{K}C_{\mathrm{BGK}}(f - f^{eq}), \tag{12}$$

where the constant $C_{\mathrm{BGK}}(\mathbf{x},t)$ might be a function of position and time but is not a function of the velocity. This model is similar to the BGK approximation for collisions used in Lattice-Boltzmann methods. It is also similar to the IEM models used in scalar mixing. In this particular context there are no theoretical justifications for this model (such as an H theorem). As the simplest possible collision model it is informative to explore its attributes. The constant C_{BGK} should always be greater than zero for a well-posed method. Unlike molecules, turbulence particles do not conserve kinetic energy when they collide, so the form of f^{eq}, the equilibrium target distribution, must be slightly different from classical theory. If we take the target distribution to be

$$f^{eq}(\hat{K}) = (\tfrac{4}{3}\pi\hat{K})^{-3/2}e^{-3v'_n v'_n/4\hat{K}}, \tag{13}$$

where $0 < \hat{K} < K$, then (as shown in Appendix A) mass and momentum are conserved and turbulent kinetic energy obeys the equation $\partial K/\partial t = -(\varepsilon/K)C_{\mathrm{BGK}}(K - \hat{K})$. This implies that $C_{\mathrm{BGK}} = 1/(1 - \hat{K}/K)$, and the dissipating collision model is

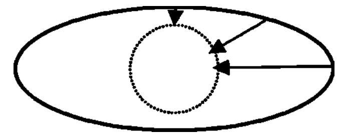

FIG. 1. BGK relaxation model. Solid line represents an isocontour for an anisotropic PDF. Dashed line is the spherical target distribution with less energy, which causes both dissipation and return-to-isotropy.

$$\frac{\partial f}{\partial t} = -\frac{\varepsilon}{(K - \hat{K})}\left(f - (\tfrac{4}{3}\pi\hat{K})^{-3/2}e^{-3v'_n v'_n/4\hat{K}}\right). \tag{14}$$

This is a model in which the PDF relaxes towards a spherical Gaussian PDF with less turbulent kinetic energy (see Fig. 1). Those portions of the PDF which are farthest from the target spherical distribution decay faster than those portions of the PDF which are closer to the target.

The equivalent Reynolds stress transport equation is obtained by multiplying by $v'_i v'_j$ and integrating over all velocities. This is shown in Appendix A, and results in the following equation:

$$\frac{\partial R_{ij}}{\partial t} = -\frac{\varepsilon}{(K - \hat{K})}(R_{ij} - \tfrac{2}{3}\hat{K}\delta_{ij}) = -\frac{\varepsilon}{K}R_{ij} - \frac{\varepsilon}{K}\frac{1}{(K/\hat{K} - 1)}(R_{ij} - \tfrac{2}{3}K\delta_{ij}). \tag{15}$$

In terms of $\hat{\Pi}$, this model is $\hat{\Pi}_{ij} = (1/[K/(\hat{K}-1)])(\delta_{ij} - \frac{2}{3}KR^{-1}_{ij})$, which is identical to the classic return model if $C_R = 1/[K/(\hat{K}-1)]$, or equivalently $\hat{K} = K[C_R/(1+C_R)]$. This implies the relation $C_{\mathrm{BGK}} = 1 + C_R = \hat{C}_R$ between the BGK relaxation constant and the Rotta constant.

From this analysis it can be seen that there is no return to isotropy if $C_R = 0$ (or $\hat{K} = 0$). Under the condition $\hat{K} = 0$, f^{eq} becomes a delta function. This observation suggests an alternative model of the form

$$\frac{\partial f}{\partial t} = -\frac{\varepsilon}{k}\big(f - \delta(v')\big) - \frac{\varepsilon}{k}C_R\big(f - f^{eq}(K)\big). \tag{16}$$

The first term (involving a delta function) produces pure decay and the second produces return to isotropy with no decay (relaxation to a spherical PDF of the same energy). This two-part model has been proposed by Degond and Lemou.[11]

While both (14) and (16) result in an identical equation for the Reynolds stress evolution (the classic linear Rotta model), the models themselves are not identical. Differences exist in the evolution of the higher turbulence moments. The model given by Eq. (16) will tend to produce a spike in the PDF around its mean value (due to the delta function). Equation (14) has a smoother influence on the PDF in general but will also produce a spike if C_R goes to zero (in the two-component or low Reynolds number limits).

Neither model has the ellipsoidal [Eq. (23)] or spherical [Eq. (18)] Gaussian as a solution. This implies that even if the turbulence starts with a Gaussian PDF it does not stay Gaussian. It is not a strict fact that turbulence should be Gaussian. Certainly under the influence of inhomogeneity we know it is not Gaussian at all. Even in homogeneous turbulence the tails of the PDF are not expected to be Gaussian. However, statistical arguments based on the central limit theorem would suggest that decaying homogeneous turbulence ought to be close to Gaussian or at least evolve in that direction for most of the core portion of the PDF. Experiments (Tavoularis and Corrsin)[20] of homogeneous turbulent shear flows support the hypothesis that homogeneous turbulence (even when sheared) has a central core that is closely approximated by an elliptical Gaussian PDF (sometimes called a trivariate normal distribution).

IV. RELAXATION COLLISION MODELS

A more general form than the BGK model [Eq. (12)] for collisions is the linear relaxation model

$$\frac{\partial f}{\partial t} = g(\mathbf{v}) - h(\mathbf{v})f, \tag{17}$$

where $g(\mathbf{v})>0$ and $h(\mathbf{v})>0$ are some positive functions of the velocity (and possibly position and time as well). The positivity requirements keep the governing equation stable and the probability always greater than zero.

In addition, the model should conserve the total probability (or mass), so that $\int g(\mathbf{v})d\mathbf{v}=\int h(\mathbf{v})fd\mathbf{v}$, and it should not cause any mean flow to be created, implying $\int v_n'[g-hf]d\mathbf{v}=0$. Finally the model should dissipate energy at the correct rate, $\int (v_n'v_n'/2)[hf-g]d\mathbf{v}=\varepsilon$.

One way to determine a suitable choice for the model functions is to insert a desired solution for the PDF function f and then derive the parameters from Eq. (17). In isotropic decaying turbulence there is evidence that the core of the PDF is very close to a Gaussian and retains this shape during the decay process (Yeung and Pope).[21] If we assume the PDF equation (17) has a Gaussian solution,

$$f(\mathbf{v},t) = (\tfrac{4}{3}\pi K)^{-3/2}e^{-3v_n'v_n'/4K}, \tag{18}$$

where $v_n'=v_n-u_n$ and u_n is the mean velocity, then taking the time derivative gives

$$\frac{\partial f}{\partial t} = \left(\frac{4}{3}\pi K\right)^{-3/2} e^{-3v_n'v_n'/4K}\left(1-\frac{v_n'v_n'}{2K}\right)\frac{3}{2}\frac{\varepsilon}{K}. \tag{19}$$

Comparing with Eq. (17) suggests that a suitable choice for the model functions is $g(\mathbf{v})=f^{eq}(\mathbf{v})(3\varepsilon/2K)$ and $h(\mathbf{v})=(3\varepsilon/2K)(v_n'v_n'/2K)$. Actually, these functions do not conserve momentum or dissipate energy at the correct rate. They must be generalized slightly to

$$\begin{aligned} g(\mathbf{v}) &= C_M\frac{3\varepsilon}{2K}\left(\frac{4}{3}\pi\hat{K}\right)^{-3/2}e^{-3\hat{v}_n'\hat{v}_n'/4\hat{K}},\\ h(\mathbf{v}) &= C_M\frac{3\varepsilon}{2K}\frac{\tilde{v}_n'\tilde{v}_n'}{[2K+(u-\tilde{u})^2]}, \end{aligned} \tag{20}$$

where we expect $C_M\to 1$, $\hat{K}\to K$, $\hat{v}_i'\to\tilde{v}_i'\to v_i'$ when the PDF approaches a spherical Gaussian [Eq. (18)]. Conservation of mass is already satisfied. Conservation of momentum implies a relationship exists between the hat and tilde velocities (see Appendix B),

$$(\hat{u}_p-u_p)[2K+(u-\tilde{u})^2] = 2R_{ip}(u_i-\tilde{u}_i)+\int v_p'v_i'v_i'fd\mathbf{v}. \tag{21}$$

This implies that either $\hat{u}_p$ or $\tilde{u}_p$ can be specified arbitrarily and then the other determined by Eq. (21). The two simplest choices are $\hat{u}_p=u_p$ which implies $\tilde{u}_i=u_i+(R_{ip}^{-1}/2)\int v_p'v_n'v_n'fd\mathbf{v}$, and $\tilde{u}_p=u_p$ which implies $\hat{u}_i=u_i+(1/2K)\int v_i'v_n'v_n'fd\mathbf{v}$. In either case, if the PDF is symmetric then the odd order integral is zero and $\tilde{u}_p=\hat{u}_p=u_p$. Since by definition $v_i=\hat{u}_i+\hat{v}_i'=\tilde{u}_i+\tilde{v}_i'=u_i+v_i'$, this also implies $\hat{v}_i'=\tilde{v}_i'=v_i'$ as well. Therefore the hat and tilde quantities in Eq. (20) can be viewed as a small perturbation imposed when the PDF is skewed (not symmetric), and are largely a formal technicality to enforce conservation of momentum.

Conservation of energy imposes a relation between C_M and $\hat{K}/K$ (Appendix B),

$$\begin{aligned}&\left[\frac{\hat{K}}{K}+\frac{1}{2K}(\hat{u}-u)^2+\frac{1}{C_M}\frac{2}{3}\right][2K+(u-\tilde{u})^2]\\ &\quad= \frac{1}{2K}\int v_p'v_p'v_i'v_i'fd\mathbf{v}+\frac{(u_p-\tilde{u}_p)}{K}\int v_p'v_i'v_i'fd\mathbf{v}\\ &\qquad+(u-\tilde{u})^2.\end{aligned} \tag{22}$$

If f is symmetric this simplifies considerably to

$$\frac{\hat{K}}{K}+\frac{1}{C_M}\frac{2}{3} = \frac{1}{4K^2}\int v_p'v_p'v_i'v_i'fd\mathbf{v}.$$

If f is an elliptic Gaussian given by

$$f = [(2\pi)^3\det(R_{nm})]^{-1/2}e^{-1/2R_{nm}^{-1}v_n'v_m'} \tag{23}$$

then the integral can be evaluated and is $4K^2+2R_{nm}R_{mn}$ (Appendix C). Then $\hat{K}/K=1+(R_{nm}R_{nm}/2K^2)-\frac{2}{3}(1/C_M)$ or perhaps even more informatively

$$\frac{3}{2}C_M = \left(1+\frac{R_{nm}R_{mn}}{2K^2}-\frac{\hat{K}}{K}\right)^{-1}.$$

The relaxation model therefore has one free parameter (either C_M or $\hat{K}/K$). Both of these parameters should go to 1 when the turbulence is isotropic (i.e., when f is a spherical Gaussian). Since $R_{nm}R_{nm}/2K^2\to\frac{2}{3}$ in isotropic turbulence, forcing one of these conditions is sufficient to guarantee the other.

The derivation of the equivalent Reynolds stress equation is given in Appendix B. The result is that Eq. (20) is equivalent to

$$\frac{\partial R_{ij}}{\partial t} = -\frac{\varepsilon}{\left[1+\dfrac{R_{nm}R_{mn}}{2K^2}-\dfrac{\hat{K}}{K}\right]}\left(\frac{R_{ij}}{K}+\frac{R_{in}R_{nj}}{K^2}-\frac{2}{3}\frac{\hat{K}}{K}\delta_{ij}\right) \tag{24}$$

if an elliptic Gaussian is assumed for the PDF shape. Equation (24) in turn implies the return parameters

$$C_R=\frac{\left[\frac{4}{3}-\frac{R_{mn}R_{nm}}{2K^2}+\frac{\hat{K}}{K}\right]}{\left[1+\frac{R_{mn}R_{nm}}{2K^2}-\frac{\hat{K}}{K}\right]}\quad\text{and}\quad C_N=\frac{-1}{\left[1+\frac{R_{mn}R_{nm}}{2K^2}-\frac{\hat{K}}{K}\right]}\tag{25}$$

or, in terms of C_M,

$$C_R=\tfrac{7}{2}C_M-1\quad\text{and}\quad C_N=-\tfrac{3}{2}C_M.\tag{26}$$

Note that this model and the other models derived in this work tend to imply that C_N is less than zero. In contrast, the widely used nonlinear model of Sarkar and Speziale[4] has a positive value for this constant. The implications of this difference are examined in detail in Sec. VIII.

Various choices of C_M are possible. The simple choice $C_M=1$ leads to $C_R=\frac{5}{2}$, and $C_N=-\frac{3}{2}$. These values produce a model which is very similar to the two models examined in detail below.

The equally simple choice $\hat{K}/K=1$ implies

$$C_R=\frac{7}{3}\frac{2K^2}{R_{nm}R_{nm}}-1\text{ and }C_N=-\frac{2K^2}{R_{nm}R_{nm}}.\tag{27}$$

This choice of $\hat{K}/K$ implies the "target" distribution has the same energy as the PDF but a spherical shape. The performance of this model is shown in Sec. V and is referred to as Model-1. The realizability condition,

$$C_R-C_N\left[\frac{R_{nk}R_{kn}}{2K^2}-\frac{4}{3}\right]=\frac{2K^2}{R_{mn}R_{nm}},$$

indicates that Model-1 is weakly realizable.

In general the realizability condition for these relaxation models is

$$C_R-C_N\left[\frac{R_{nk}R_{kn}}{2K^2}-\frac{4}{3}\right]=\frac{\hat{K}}{K}\bigg/\left(1+\frac{R_{nm}R_{mn}}{2K^2}-\frac{\hat{K}}{K}\right),$$

so choices where $\hat{K}/K$ vanish in the two-component limit will satisfy the strong realizability condition. The quantity $F=\det(R_{ij})/(\frac{2}{3}K)^3$ is 1 in isotropic turbulence and 0 in the two component limit. The choice $\hat{K}/K=F$ means that

$$C_R=\frac{\left[\frac{4}{3}-\frac{R_{mn}R_{nm}}{2K^2}+F\right]}{\left[1+\frac{R_{mn}R_{nm}}{2K^2}-F\right]}\text{ and }C_N=\frac{-1}{\left[1+\frac{R_{mn}R_{nm}}{2K^2}-F\right]}.\tag{28}$$

The other strong realizability condition ($C_N\geqslant -2K^2/R_{nm}R_{mn}$ when $F=0$) is also satisfied by this model. Referred to as Model-F, the performance of this model is also shown in Sec. V. This model has a target distribution that has less energy, and in this sense it is similar to the simple BGK model of Sec. III. However, unlike the BGK model, this model has the spherical Gaussian as a solution, is strongly realizable and does not produce a spike in the PDF in the two-component limit. In addition, unlike the simple BGK model, the decay constant h now depends on the velocity $\mathbf{v}$ and acts preferentially on the tails of the distribution, damping extreme events more strongly. While there is one free-parameter left in this model, $\hat{K}/K$, it is far more restricted in its behavior than the arbitrary constant $C_{\mathrm{BGK}}=1+C_R=\hat{C}_R$ found in the simpler BGK type relation model. All possible choices for $\hat{K}/K$ that have been tried (three so far) give very similar results for the actual model predictions, so this type of model is far less "tunable."

V. MODEL PERFORMANCE

In this section the performance of these models is compared with experimental data for return to isotropy. For each test case, we present both the Reynolds stresses as a function of time and the Reynolds stress anisotropy as a function of time. The anisotropy is the standard method for looking at return-to-isotropy, since it eliminates much of the dependence on the dissipation. However, due to the nondimensionalization with respect to K the anisotropy can cause errors in one turbulence component (possibly even experimental errors) to appear as a general failure of the entire model. For this reason we retain the direct Reynolds stress decay plots as well.

In all models the dissipation is determined from the model transport equation

$$\frac{\partial\varepsilon}{\partial t}=-C_{\varepsilon 2}\frac{\varepsilon^2}{K}.\tag{29}$$

The value of $C_{\varepsilon 2}$ is taken to be 11/6, which is the high Reynolds number analytical solution for turbulence with a low wavenumber k^2 spectrum.[22] In most of the experiments the initial value of the dissipation is not known, and is obtained by attempting to match the K profile as well as possible.

In each case, we have solved the Reynolds stress ordinary differential equation (ODE) associated with the model, using fourth order Runge–Kutta and very small time steps. We have also solved the corresponding PDF relaxation models and obtained very similar results. However, there are further numerical issues associated with solving the PDF equations which we do not wish to address here, so we simply present the ODE results in this paper.

Because $C_{\varepsilon 2}$ and the return process are believed to be Reynolds number dependent, we have selected only high Re number experiments for comparison and no direct numerical simulation (DNS) test cases. It must be noted that there is some uncertainty associated with the experimental results. First, while the geometry of these experiments changes abruptly from a straining section to a straight section, the actual cessation of the mean strain may not be quite so abrupt due to the long range effects of pressure. As a result, these decay experiments may have some residual straining in them at early times. The translation of the zero time in the Le Penven experiment, case III$<$0, suggests that the experimenters were aware of this problem. More importantly, the initial turbulence for these experiments has structure, due to the strains imposed to make the turbulence anisotropic. It is likely that at early times the relaxation of these structures also affects the return process.

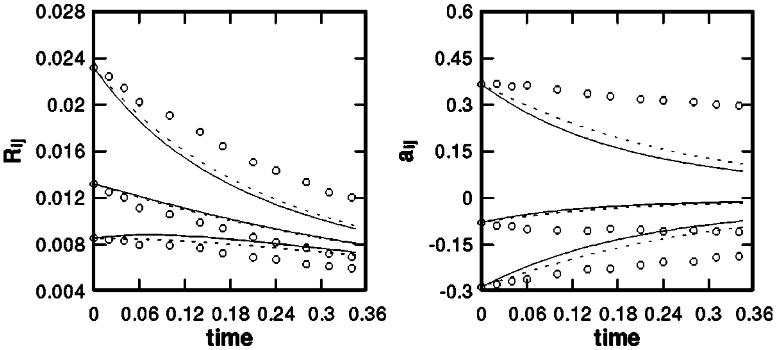

FIG. 2. Reynolds stresses and anisotropy for the case III>0 from Le Penven, Gence, and Comte-Bellot. Symbols are the experimental data, lines are the Model-1 predictions, and the dashed lines are the Model-F predictions.

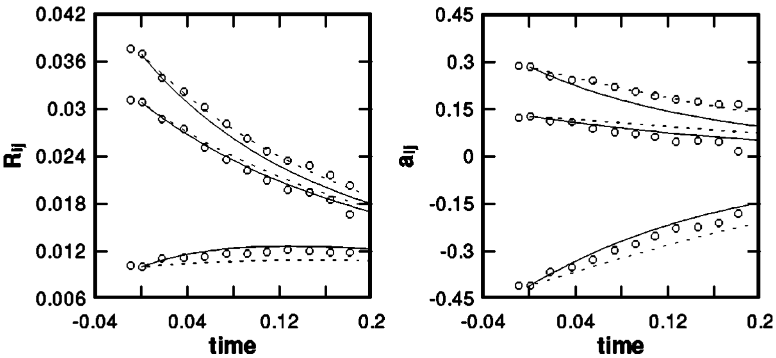

FIG. 3. Reynolds stresses and anisotropy for case III <0 from Le Penven, Gence, and Comte-Bellot. Symbols are the experimental data, lines are the Model-1 predictions, and the dashed lines are the Model-F predictions.

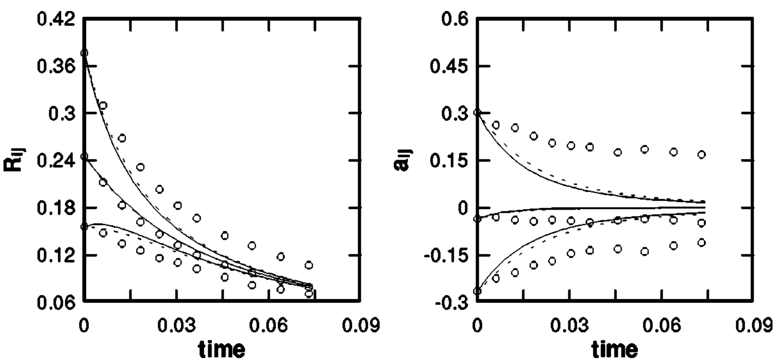

FIG. 4. Reynolds stresses and anisotropy for case A of Choi and Lumley. Symbols are the experimental data, lines are the Model-1 predictions, and the dashed lines are the Model-F predictions.

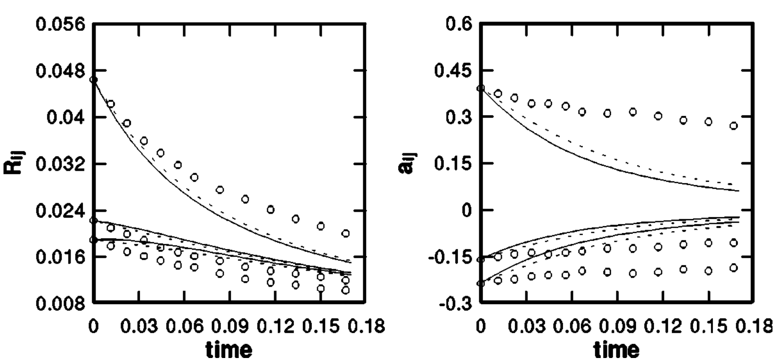

FIG. 5. Reynolds stresses and anisotropy for case B of Choi and Lumley. Symbols are the experimental data, lines are the Model-1 predictions, and the dashed lines are the Model-F predictions.

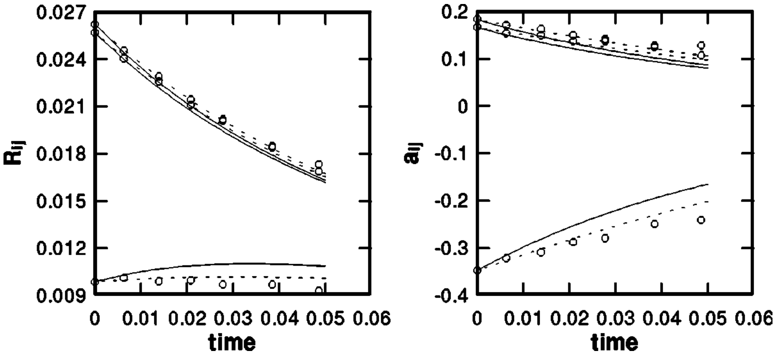

FIG. 6. Reynolds stresses and anisotropy for case C-2 of Choi and Lumley. Symbols are the experimental data, lines are the Model-1 predictions, and the dashed lines are the Model-F predictions.

Figures 2 and 3 are Le Penven *et al.* cases III >0 (expansion) and III <0 (contraction). Figures 4–6 are the data of Choi and Lumley[7] for their cases A (plane distortion), B (axisymmetric expansion), and C-2 (axisymmetric contraction), respectively.

Despite the fact that model-F is strongly realizable and Model-1 is not, the two models behave very similarly for all five experimental test cases. With the exception of Fig. 3 (Le Penven, case III <0) and Fig. 6 (Choi and Lumley, case C-2) the models show poor agreement with the experimental data, and tend to return to isotropy too quickly.

VI. GENERAL RELAXATION MODELS

Rather than assuming a spherical Gaussian, let us assume that the anisotropic ellipsoidal Gaussian [Eq. (23)] is a solution to the relaxation equation [Eq. (17)]. It will ultimately be seen that this gives much better model predictions. With this very broad assumption,

$$\frac{\partial f}{\partial t} = -\frac{1}{2} f\left(\frac{\partial/\partial t \det(R_{nm})}{\det(R_{nm})} + \frac{\partial R_{nm}^{-1}}{\partial t} v_n' v_m'\right). \tag{30}$$

Since $\partial R_{ij}^{-1}/\partial t = -R_{im}^{-1}(\partial R_{mn}/\partial t)R_{nj}^{-1}$ and $\partial/\partial t \det(R_{nm}) = \det(R_{nm})(\partial R_{ip}/\partial t)R_{pi}^{-1}$ (Jacobi's formula) this reduces to

$$\frac{\partial f}{\partial t} = -\frac{1}{2} f(R_{ij}^{-1} - R_{im}^{-1}R_{nj}^{-1}v_n' v_m')\frac{\partial R_{ij}}{\partial t}. \tag{31}$$

Let us further assume that $\partial R_{ij}/\partial t = -\varepsilon/2K(\Pi_{im}R_{mj} + \Pi_{jm}R_{mi})$ which is the general Reynolds stress transport model [Eq. (5)]. Then

$$\frac{\partial f}{\partial t} = \frac{\varepsilon}{2K} f\left(\Pi_{ii} - \Pi_{in}R_{im}^{-1}v_m' v_n'\right). \tag{32}$$

This implies that for any desired Reynolds stress model Π_{ij} a corresponding relaxation model can be constructed,

$$g(\mathbf{v}) = C_M \Pi_{ii} \frac{\varepsilon}{2K} \frac{e^{-1/2\hat{R}_{nm}^{-1}\hat{v}_n'\hat{v}_m'}}{[(2\pi)^3 \det(\hat{R}_{nm})]^{1/2}},$$
$$h(\mathbf{v}) = C_M \frac{\varepsilon}{2K} \frac{\Pi_{in}R_{im}^{-1}\tilde{v}_m'\tilde{v}_n'}{\left[1 + (u_n - \tilde{u}_n)(u_m - \tilde{u}_m)R_{im}^{-1}\frac{\Pi_{in}}{\Pi_{pp}}\right]}. \tag{33}$$

When the PDF is an elliptic Gaussian we expect $C_M = 1$, $\tilde{v}_n' = \hat{v}_n' = v_n'$, and $\hat{R}_{nm} = R_{nm}$. The constant C_M can be a function of tilde and hat quantities (such as $\tilde{u}_p - u_p$ and $\hat{u}_p - u_p$) but it can no longer be a function of the Reynolds stress invariants (like it was in the simpler spherical relaxation model). This is because the elliptic Gaussian PDF (unlike the spherical Gaussian PDF) can represent any state of the Reynolds stress invariants.

Note that the relaxation equation places constraints on the underlying Reynolds stress model. It implies that $\Pi_{ii} > 0$, and $\Pi_{in}R_{im}^{-1}$ must be a positive definite tensor.

Conservation of probability (or mass) is already satisfied by this model. Conservation of momentum requires a relation between $\hat{u}_p$ and $\tilde{u}_p$ (see Appendix D),

$$(\hat{u}_p - u_p)\left[1 + (u_n - \tilde{u}_n)(u_m - \tilde{u}_m)R_{im}^{-1}\frac{\Pi_{in}}{\Pi_{pp}}\right] = \frac{\Pi_{in}}{\Pi_{ii}}R_{im}^{-1}\left\{\int v_p' v_m' v_n' f d\mathbf{v} + R_{np}(u_m - \tilde{u}_m) + R_{mp}(u_n - \tilde{u}_n)\right\}. \tag{34}$$

The simplest choice is $\tilde{u}_p = u_p$ then

$$\hat{u}_p = u_p + \frac{\Pi_{in}}{\Pi_{ii}}R_{im}^{-1}\int v_p' v_m' v_n' f d\mathbf{v}. \tag{35}$$

The choice $\hat{u}_p = u_p$ is more complicated and requires a symmetric matrix inversion $(\Pi_{ip}R_{in}^{-1} + \Pi_{in}R_{ip}^{-1})(\tilde{u}_n - u_n) = \Pi_{in}R_{im}^{-1}R_{tp}^{-1}\int v_t' v_m' v_n' f d\mathbf{v}$. For certain models (like the one shown below), this matrix problem is easy to invert analytically, and this choice is also viable.

The Reynolds stress transport equation is derived in Appendix E. Assuming the choice $\tilde{u}_p = u_p$ it requires that

$$\hat{R}_{ij} = \frac{\Pi_{pn}}{\Pi_{ss}}R_{pm}^{-1}\int v_m' v_n' v_i' v_j' f d\mathbf{v} - \frac{1}{C_M}\left(\frac{\Pi_{im}}{\Pi_{ss}}R_{mj} + \frac{\Pi_{jm}}{\Pi_{ss}}R_{mi}\right) - (\hat{u}_i - u_i)(\hat{u}_j - u_j). \tag{36}$$

If the PDF is an ellipsoidal Gaussian then $\hat{u}_p = u_p$ [by Eq. (35)], and $C_M = 1$ (by definition). In addition, since

$$\int v_m' v_n' v_i' v_j' f d\mathbf{v} = R_{mn}R_{ij} + R_{mi}R_{nj} + R_{mj}R_{ni} \tag{37}$$

Eq. (36) gives the correct limit, $\hat{R}_{ij} = R_{ij}$ for an elliptic Gaussian PDF. The hat and tilde quantities can be seen to be slight perturbations to the standard quantities that precisely account for any deviation of the PDF from an elliptic Gaussian shape.

The model given by Eqs. (33)–(36) represents the general relaxation model. Using this formulation, any Reynolds stress transport model can also be implemented as a PDF relaxation model, which has the elliptic Gaussian as a solution. Remember that $\Pi_{ij}=\delta_{ij}$ corresponds to the case of no return-to-isotropy, and $\Pi_{ij}=\delta_{ij}+C_R(\delta_{ij}-\frac{2}{3}KR_{ij}^{-1})$ is the classic linear return-to-isotropy model. Substituting these expressions into Eqs. (33)–(36) will produce the corresponding PDF relaxation model. However, in this paper, we do not wish to specify Π_{ij}, but to determine what the general relaxation model [Eqs. (33)–(36)] imply about how it should be specified.

The general relaxation model as described above has singular h, $\hat{u}_p$, and $\hat{R}_{ij}$ in the two-component limit due to the presence of R_{ij}^{-1}. This singularity is removed by the parameter-free Reynolds stress model $\Pi_{ij}=(2K/R_{\mathrm{nm}}R_{\mathrm{mn}})R_{ij}$. Making Π_{ij} directly proportional to the Reynolds stress tensor removes the singularities. The constant of proportionality is determined from the decay condition $\Pi_{ij}R_{ij}=2K$ (see Sec. III). In the relaxation context this model is given by

$$g = C_M\frac{\varepsilon}{K}\frac{2K^2}{R_{nm}R_{mn}}\frac{e^{-1/2\hat{R}_{nm}^{-1}\hat{v}_n'\hat{v}_m'}}{[(2\pi)^3\det(\hat{R}_{nm})]^{1/2}},$$
$$h = C_M\frac{\varepsilon}{K}\frac{2K^2}{R_{nm}R_{mn}}\frac{\tilde{v}_n'\tilde{v}_n'}{[2K+(u-\tilde{u})^2]}, \tag{38}$$

where

$$(\hat{u}_p-u_p)[2K+(u-\tilde{u})^2] = 2R_{ip}(u_i-\tilde{u}_i)+\int v_p'v_i'v_i'fd\mathbf{v}. \tag{39}$$

Note that Eq. (39) is a particular case of the general Eq. (34) (for this Π_{ij} model). It also happens to be identical to Eq. (21), the general expression for the spherical relaxation models in Sec. IV. As in Sec. IV, the choice of $\hat{u}_p=u_p$ or $\tilde{u}_p=u_p$ is up to the user. For symmetric PDFs it makes no difference what the choice is, since then $\hat{u}_p=\tilde{u}_p=u_p$. For inhomogeneous flows, the PDFs will be skewed and this choice may make some difference.

For this model we also require the condition on $\hat{R}_{ij}$ that

$$\left[\hat{R}_{ij}+(\hat{u}_i-u_i)(\hat{u}_j-u_j)+\frac{1}{C_M}\frac{R_{im}R_{mj}}{K}\right][2K+(u-u)^2]$$
$$=\int v_n'v_n'v_i'v_j'fd\mathbf{v}+(u_n-u_n)\int v_n'v_i'v_j'fd\mathbf{v}+R_{ij}(u-u)^2. \tag{40}$$

This model [Eqs. (38)–(40)] differs from those in Sec. IV, in that it has the ellipsoidal Gaussian as a solution.

The choices for C_M are now far more restrictive. The simplest choice is simply to set $C_M=1$. Equations (40) and (39) are simplified considerably by choosing $\tilde{u}_p=u_p$. Then the hat quantities are defined by $\hat{u}_p=u_p+(1/2K)\int v_p'v_i'v_i'fd\mathbf{v}$ and $\hat{R}_{ij}=(1/2K)\int v_n'v_n'v_i'v_j'fd\mathbf{v}-(\hat{u}_i-u_i)(\hat{u}_j-u_j)-(1/C_M)(R_{im}R_{mj}/K)$.

The equivalent Reynolds stress transport model can be derived from this relaxation model by assuming the PDF is an elliptic Gaussian. Under this assumption, the various possible choices of the hat and tilde quantities are irrelevant and we find that all these choices are equivalent to

$$\frac{\partial R_{ij}}{\partial t} = -2\varepsilon\frac{R_{is}R_{sj}}{R_{mn}R_{nm}}, \tag{41}$$

which implies the model parameters are

$$C_R = \frac{4}{3}\frac{2K^2}{R_{mn}R_{nm}}-1 \text{ and } C_N = -\frac{2K^2}{R_{mn}R_{nm}}. \tag{42}$$

We note that this model satisfies the strong realizability constraint, $C_R-C_N[R_{nk}R_{kn}/(2K^2)-\frac{4}{3}]=0$, and sits on the cusp of the strong realizability condition $C_N\geqslant-2K^2/R_{mn}R_{nm}$. In the two-component limit, this model returns to isotropy as slowly as physically possible. The performance of this model is shown below and it is referred to as Model-EG (for elliptic Gaussian). The fact that the resulting Reynolds stress model is very simple, entirely nonlinear, contains no model parameters, and satisfies strong realizability at its cusp, makes Model-EG very intriguing.

In Figs. 7–11 the performance of Model-EG is compared with experimental data for return-to-isotropy, the classic linear Rotta model (with $C_R=0.8$), and the nonlinear model of Sarkar and Speziale ($C_R=0.7$, $C_N=1.05$). The most interesting result is that these three very different models perform very similarly for all five test cases. The Sarkar and Speziale model is slightly better than the other two, but it has two adjustable model constants that were tuned to exactly these test cases. The linear Rotta model also performs surprisingly well. It can be made even better by adjusting the standard value (0.8) downwards (to 0.7 or 0.6). Model-EG matches the data the least well, but gives quite good agreement considering there are no adjustable parameters in this model.

As noted earlier, the greatest uncertainty in both the models and the experiments lies in the initial conditions. To see that the assessment of the models performance is not affected by these initial conditions, Fig. 8 was recalculated using a later time for initialization. Figure 12 shows that the point of initialization does not fundamentally change the results.

We conclude this section by noting that other return models have been proposed that are nonlinear, which parameterize C_R and C_N as functions of the Reynolds stress invariants (or anisotropy invariants), and which satisfy strong realizability.[7,17] However, these models assume that C_R and C_N are polynomial functions of the invariants. In contrast, the model described above uses linear *rational* polynomial functions of the invariants to represent the return parameters C_R and C_N. We note that rational polynomials tend to have better fitting properties than polynomials, and that the formulated rational polynomials are the result of physical assumptions but not assumptions about functional behavior.

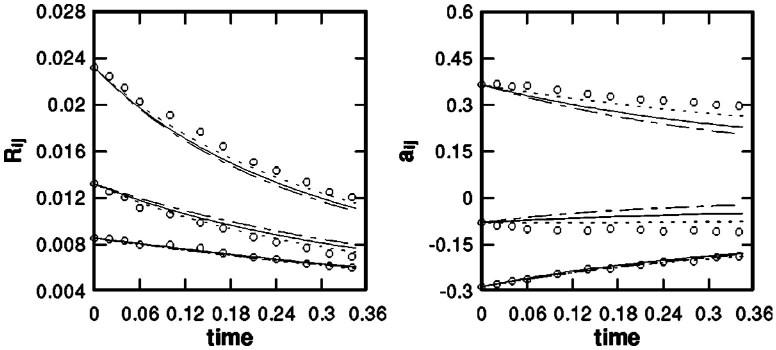

FIG. 7. Reynolds stresses and anisotropy for the case III>0 from Le Penven, Gence, and Comte-Bellot. Symbols are the experimental data, lines are the Rotta model predictions (C_R=0.8), the dashed lines are the SS model predictions, and large dashed lines are the Model-EG predictions.

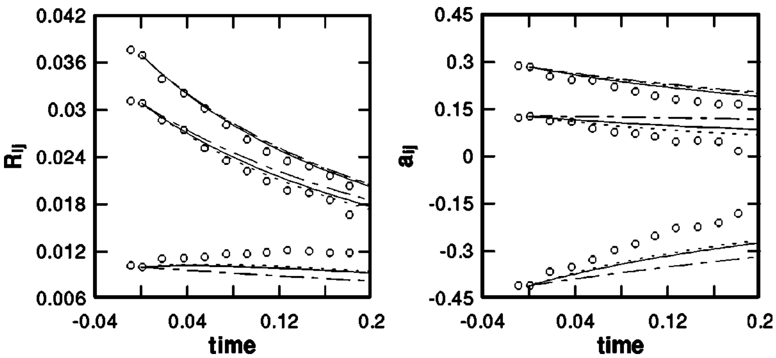

FIG. 8. Reynolds stresses and anisotropy for case III <0 from Le Penven, Gence, and Comte-Bellot. Symbols are the experimental data, lines are the Rotta model predictions (C_R=0.8), the dashed lines are the SS model predictions, and large dashed lines are the Model-EG predictions.

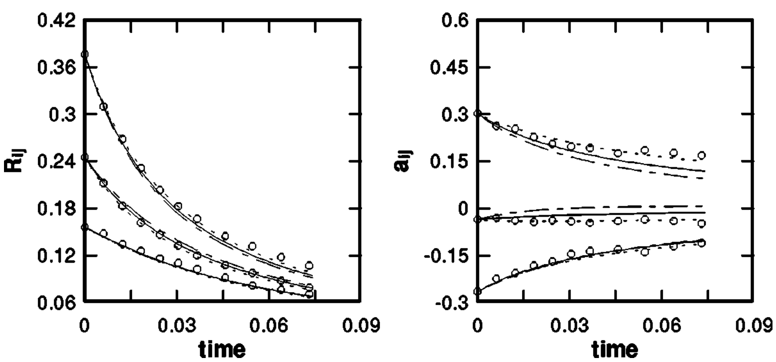

FIG. 9. Reynolds stresses and anisotropy for case A of Choi and Lumley. Symbols are the experimental data, lines are the Rotta model predictions (C_R=0.8), the dashed lines are the SS model predictions, and large dashed lines are the Model-EG predictions.

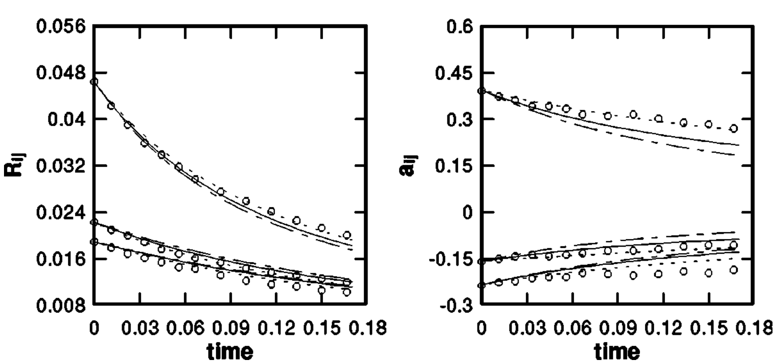

FIG. 10. Reynolds stresses and anisotropy for case B of Choi and Lumley. Symbols are the experimental data, lines are the Rotta model predictions (C_R=0.8), the dashed lines are the SS model predictions, and large dashed lines are the Model-EG predictions.

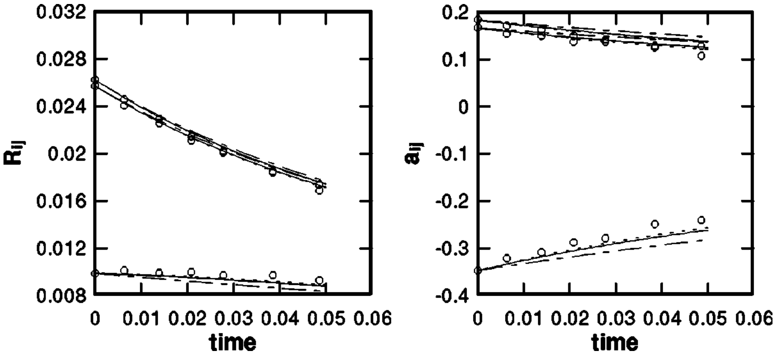

FIG. 11. Reynolds stresses and anisotropy for case C-2 of Choi and Lumley. Symbols are the experimental data, lines are the Rotta model predictions (C_R=0.8), the dashed lines are the SS model predictions, and large dashed lines are the Model-EG predictions.

VII. FOKKER–PLANCK COLLISION MODELS

An alternative to relaxation models is the Fokker–Planck collision model. This model is frequently used to model Brownian motion, liquid collisions, and some plasmas. Langevin models for turbulence[19,23] are directly related to the Fokker–Planck equation and therefore effectively use this type of model. A generalized Fokker–Planck collision operator involves two as yet unspecified matrices, G_{ij} and H_{ij},

$$-\frac{\partial f}{\partial t} = -\frac{\partial (G_{ij} v_j' f)}{\partial V_i} + \frac{\partial}{\partial V_i}\left[H_{ij}\frac{\partial f}{\partial V_j}\right]. \tag{43}$$

The tensor H_{ij} should be positive definite for stability reasons. In Langevin models it is convenient to make H_{ij} isotropic as well. However, in general the Fokker–Planck collision model has considerable flexibility in the choice of both the model tensors. The model automatically satisfies conservation of probability and momentum. It also has the ellipsoidal Gaussian as a solution.[24] Multiplying Eq. (43) by $v_n' v_m'$ and integrating over all velocity space gives the equivalent Reynolds stress transport equation

$$\frac{\partial R_{nm}}{\partial t} = G_{mj}R_{jn} + G_{nj}R_{jm} + H_{mn} + H_{nm}. \tag{44}$$

By comparing this with the generic Reynolds stress transport equation [Eq. (5)], it can be seen that

$$G_{ij} + H_{im}R_{mj}^{-1} = -\frac{\varepsilon}{2K}\Pi_{ij}. \tag{45}$$

In this way, classic return models (given in terms of Π_{ij}) can be implemented in the generalized Fokker–Planck context. This transformation is also discussed in Pope.[19] The general nonlinear Reynolds stress return model [Eq. (8)] is equivalent to

$$\Pi_{ij} = \delta_{ij} + \left\{ C_R + C_N\left[\frac{4}{3} - \frac{R_{nk}R_{kn}}{2K^2}\right]\right\}(\delta_{ij} - \tfrac{2}{3}KR_{ij}^{-1}) - C_N\left(\frac{R_{ij}}{K} - \frac{R_{nk}R_{kn}}{2K^2}\delta_{ij}\right). \tag{46}$$

In the Fokker–Planck context this implies that

$$G_{ij} + H_{im}R_{mj}^{-1} = -\frac{\varepsilon}{2K}\left[\delta_{ij} + \left\{C_R + C_N\left[\frac{4}{3} - \frac{R_{nk}R_{kn}}{2K^2}\right]\right\} \times(\delta_{ij} - \tfrac{2}{3}KR_{ij}^{-1}) - C_N\left(\frac{R_{ij}}{K} - \frac{R_{nk}R_{kn}}{2K^2}\delta_{ij}\right)\right]. \tag{47}$$

There are many possible choices of G_{ij} and H_{ij} which satisfy this constraint.

The simplest and most numerically attractive choice for H_{ij} is that this tensor is isotropic, $H_{ij}=C_D\varepsilon\delta_{ij}$, where C_D is an arbitrary model constant. This means that

$$G_{ij} = -\frac{\varepsilon}{2K}\left[(1 + C_R + \frac{4}{3}C_N)\delta_{ij} - C_N\frac{R_{ij}}{K}\right] + \frac{\varepsilon}{3}\left(C_R + C_N\left[\frac{4}{3} - \frac{R_{nk}R_{kn}}{2K^2}\right] - 3C_D\right)R_{ij}^{-1}. \tag{48}$$

The singularity in G_{ij} is removed by the particular choice $3C_D = C_R + C_N\left[\frac{4}{3} - (R_{nk}R_{kn}/2K^2)\right]$, which is the choice used in

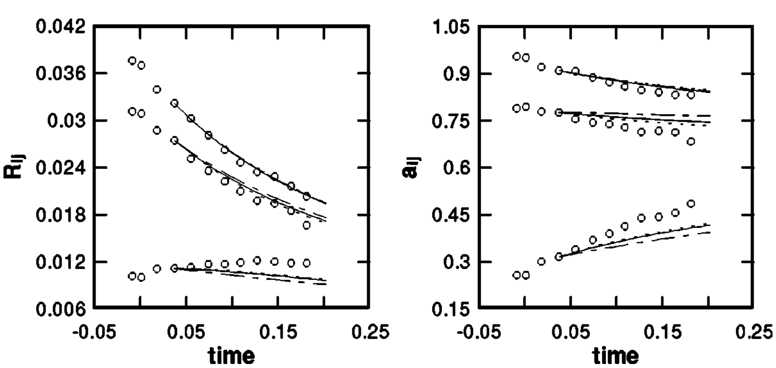

FIG. 12. Reynolds stresses and anisotropy for the case III<0 from Le Penven, Gence, and Comte-Bellot, initialized at 0.037. Symbols are the experimental data, lines are the Rotta model predictions (C_R=0.8), the dotted lines are the SS model predictions, and dashed lines are the Model-EG predictions.

most Langevin turbulence models. This gives the following model constants:

$$H_{ij} = \left[C_R + C_N\left(\frac{4}{3} - \frac{R_{nk}R_{kn}}{2K^2}\right)\right]\frac{\varepsilon}{3}\delta_{ij}$$

and

$$G_{ij} = -\frac{\varepsilon}{2K}\left[(1+C_R)\delta_{ij} + C_N\left(\frac{4}{3}\delta_{ij} - \frac{R_{ij}}{K}\right)\right]. \tag{49}$$

Note that with this choice the weak realizability constraint $C_R + C_N[\frac{4}{3} - (R_{nk}R_{kn}/2K^2)] \geqslant 0$ is equivalent to the requirement that H_{ij} be positive definite. Under these circumstances, the classic linear return model (with $C_N=0$) is obtained using $G_{ij}=-(\varepsilon/2K)(1+C_R)\delta_{ij}$ and $H_{im}=(\varepsilon/3)C_R\delta_{im}$. Model-1 given in Sec. IV [with $C_R=\frac{7}{3}(2K^2/R_{nk}R_{kn})-1$ and $C_N=-2K^2/R_{nk}R_{kn}$] is obtained using

$$H_{ij} = \left(\frac{2K^2}{R_{nk}R_{kn}}\right)\frac{\varepsilon}{3}\delta_{ij} \text{ and } G_{ij} = -\frac{\varepsilon}{2K}\left(\frac{2K^2}{R_{nk}R_{kn}}\right)\left[\delta_{ij} + \frac{R_{ij}}{K}\right].$$

Model-F, with

$$C_R = \frac{\left[\frac{4}{3} - \frac{R_{mn}R_{nm}}{2K^2} + F\right]}{\left[1 + \frac{R_{mn}R_{nm}}{2K^2} - F\right]} \text{ and } C_N = \frac{-1}{\left[1 + \frac{R_{mn}R_{nm}}{2K^2} - F\right]},$$

is obtained using

$$H_{ij} = \frac{\varepsilon}{3}\delta_{ij}F \bigg/ \left[1 + \frac{R_{mn}R_{nm}}{2K^2} - F\right]$$

and

$$G_{ij} = -\frac{\varepsilon}{2K}\left[\delta_{ij} + \frac{R_{ij}}{K}\right] \bigg/ \left[1 + \frac{R_{mn}R_{nm}}{2K^2} - F\right].$$

Note that in the two-component limit H_{ij} now goes to zero. This particular splitting [Eq. (7.7)] will be unstable in this limit. Model-EG, with

$$C_R = \frac{4}{3}\frac{2K^2}{R_{mn}R_{nm}} - 1 \text{ and } C_N = -\frac{2K^2}{R_{mn}R_{nm}},$$

is obtained using $H_{ij}=0$ and

$$G_{ij} = -\frac{\varepsilon}{2K}\left(\frac{2K^2}{R_{mn}R_{nm}}\right)\frac{R_{ij}}{K}.$$

This model is therefore incompatible with this splitting (unstable). If H_{ij} is assumed to be isotropic (and nonzero), then G_{ij} must become singular in the two-component limit.

A more general splitting is possible if H_{ij} is allowed to be anisotropic. Classic Langevin models require isotropic H_{ij}, but the Fokker–Planck model itself only requires H_{ij} to be positive definite. Assuming a positive definite form, $H_{ij}=C_D\varepsilon\delta_{ij}+C_E(\varepsilon/K)R_{ij}$ implies

$$G_{ij} = -\frac{\varepsilon}{2K}(1 + C_R + \frac{4}{3}C_N + 2C_E)\delta_{ij} + (C_S - 3C_D)\frac{\varepsilon}{3}R_{ij}^{-1} + C_N\frac{\varepsilon}{2K^2}R_{ij}, \tag{50}$$

where $C_S=C_R+C_N(\frac{4}{3}-R_{nk}R_{kn}/2K^2)$. Again, to remove the near singularity $C_D=\frac{1}{3}C_S$ can be chosen, but because of the more general form for H_{ij} the (realizability) restriction $C_S \geqslant 0$ is no longer required for a well-posed model. The classic linear return model is obtained using $G_{ij}=-(\varepsilon/2K)(1+C_R+2C_E)\delta_{ij}$ and $H_{im}=(\varepsilon/3)C_R\delta_{im}+C_E(\varepsilon/K)R_{ij}$. Note that this splitting has an extra free parameter C_E which does not change the Reynolds stress evolution, but does change the model. A nonsingular splitting for Model-EG, with

$$C_R = \frac{4}{3}\frac{2K^2}{R_{nk}R_{kn}} - 1 \quad \text{and} \quad C_N = -\frac{2K^2}{R_{nk}R_{kn}},$$

is now given by

$$G_{ij} = -\frac{\varepsilon}{R_{nk}R_{kn}}R_{ij} - \frac{\varepsilon}{K}C_E\delta_{ij} \quad \text{and} \quad H_{ij} = \frac{\varepsilon}{K}C_E R_{ij},$$

where C_E is again an arbitrary parameter. Note that C_E can actually be determined by a dispersion analysis and is related to the Kolmorgorov constant.

VIII. DISCUSSION

The return-to-isotropy problem of anisotropic turbulence has been studied via three very different collision models for the evolution of the velocity PDF. The simplest collision operator is the BGK approximation to the Boltzmann collision integral. This collision model, $(-\varepsilon/k)C_{\text{BGK}}(f-f^{eq})$, is characterized by an inverse time scale (which does not depend on the velocity). It was shown that if this model is to dissipate energy correctly, the target state must have considerably less energy than the current PDF state. Some models even use a target state with zero energy (a delta function). The BGK model produces the classic linear return-to-isotropy model, with the rate of return $C_R=1/(K/\hat{K}-1)$ determined by the energy of the target state. The Gaussian PDF is not a solution of the BGK model even though theoretical and experimental evidence might suggest that this is desirable.

To overcome the limitations of the BGK model, more general relaxation models were constructed in which the collision operator $g(v)-h(v)f$ has a positive-definite velocity dependent source term and a velocity dependent sink term that is proportional to the PDF. Previous analysis of this collision model in the context of turbulence is unknown to the authors. In Sec. IV prescriptions for the model parameters g and h were derived such that the spherical Gaussian is a solution to the evolution equation. Two models were derived from this analysis, Model-1 assumed that the target distribution has the same energy as the PDF, $\hat{K}/K=1$. It is only weakly realizable. Model-F assumed that the target distribution has less energy than the PDF in the ratio $\hat{K}/K=F$. This ratio was chosen because it makes the resulting model strongly realizable. While these initial parameter-free relax-

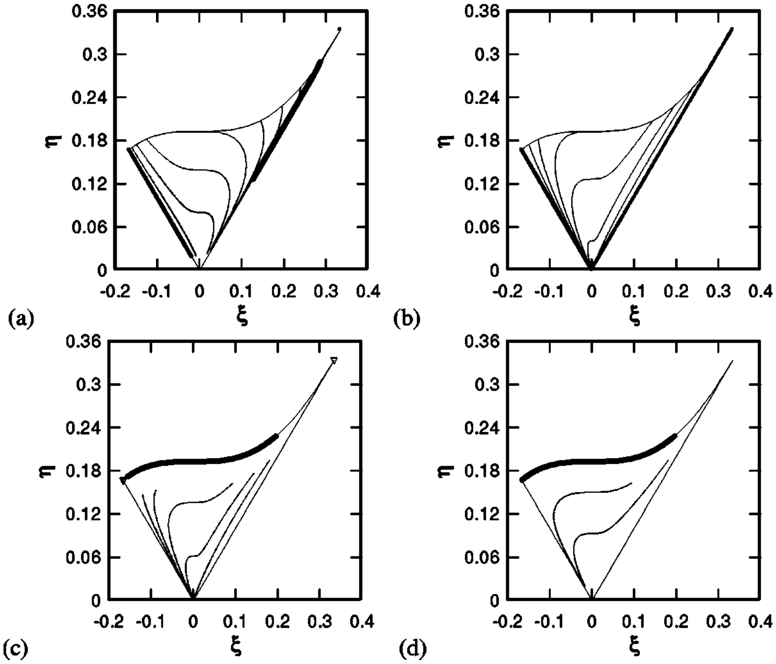

FIG. 13. Invariant triangle. (a) Sarkar and Speziale, (b) Model-1, (c) Model-F, (d) Model-EG.

ation models did not perform as well as might be hoped, they set the stage for the development of the parameter-free Model-EG.

Model-EG was shown to be the only nonsingular relaxation model that has the elliptic Gaussian as a solution. The equivalent Reynolds stress transport model is totally nonlinear in the Reynolds stresses and was shown to be strongly realizable. Interestingly, the performance of Model-EG is quite similar to the linear return to isotropy model. Even the Sarkar and Speziale model with an opposite sign for the nonlinear term, C_N, performs similarly for the test cases studied.

To investigate these models further, their trajectories on the anisotropy invariant map were plotted, and are presented in Fig. 13. It is well known that the linear Rotta model has linear trajectories when plotted on this anisotropy invariant map. The trajectories of the model of Sarkar and Speziale tend to move downwards and from left to right on this map. This means that turbulence with two large Reynolds stresses and one small stress will tend to first approach a state with only one large stress before approaching full isotropy. This implies that the intermediate stress decays faster than the maximum and minimum stresses, which is somewhat counter intuitive. The models developed in this paper tend to have the opposite behavior. Turbulence with one large stress will first decay to a state with two large stresses before approaching total isotropy. There is no experimental data in the middle of the triangle that allows us to determine which behavior is actually correct.

The top boundary of the "triangle" is the two-component line. The strongly realizable models have trajectories that stay on this line and move to the left if they start on the two-component line. This means that if one component of the turbulence is zero it stays zero for all time, and the two nonzero stresses approach each other (mutual isotropy). This is the expected behavior for two-dimensional turbulence, which is sometimes (but by no means always) found when the turbulence is two component. More information about the turbulence (than the Reynolds stress) is clearly necessary to make return models behave correctly in the two-component limit. Strong realizability seems appropriate when the two-component turbulence is also two dimensional, and weak realizability seems appropriate otherwise.

Finally, the relationship between the relaxation models and the Fokker–Planck collision model

$$\left(-\frac{\partial(G_{ij}v_j'f)}{\partial V_i}+\frac{\partial}{\partial V_i}H_{ij}\frac{\partial f}{\partial V_j}\right)$$

was investigated. Like the general relaxation model (Sec. VI) the Fokker–Planck model has the ellipsoidal Gaussian as a solution. Because it involves derivatives in velocity space, the Fokker–Planck model is more difficult to implement numerically than relaxation models. However, the Fokker–Planck model (with isotropic H_{ij}) has a direct correspondence with the Langevin PDF models. Examination of Model-EG in this context showed that this model cannot be implemented with isotropic H_{ij}. Instead, the diffusion coefficient H_{ij} must be proportional to R_{ij}.

In this work, fairly reasonable assumptions have been explored for how large collections of interacting dissipative particles (turbulent eddies) might be expected to behave. We have then explored the modeling implications of these assumptions, and then tested against experimental data and theoretical analysis (realizability considerations) to determine which assumptions are the most reasonable. The models are therefore telling us information about the physics.

The primary assumption has been that turbulence tends toward a spherical or an elliptic Gaussian PDF distribution. While it is not entirely clear that high Reynolds number decaying anisotropic turbulence should become Gaussian (spherical or elliptic), these are certainly very reasonable and relatively broad starting points. The evidence from this paper indicates that turbulence does not try to approach a spherical Gaussian (except in the limit as time goes to infinity). However we have found that models that assume that the ellipsoidal Gaussian distribution is a solution appear to have very interesting predictive and theoretical properties. In particular, we have determined the unique nonsingular (assuming nature abhors a singularity) model of this form. The equivalent Reynolds stress transport model [Eq. (41)] has not been proposed in the past but does have a number of attractive predictive and theoretical properties. In particular, and probably most importantly for many modelers, this model (in its transport equation form) has absolutely no tunable constants. Less useful, but perhaps just as interesting, this model cannot be implemented as a classical Lagrangian PDF method (Langevin equation).

ACKNOWLEDGMENTS

The authors gratefully acknowledge the financial support of this work by the Office of Naval Research (Grant Nos. N00014-01-1-0483 and N00014-04-1-0267) under the supervision of Dr. Ronald Joslin.

APPENDIX A: BHATNAGAR–GROSS–KROOK MOMENTS

Conservation of mass (or probability) requires that the integral of the PDF be equivalent to one for all time. This means that the integral of its time derivative must be zero. Starting from the BGK model for the time derivative of distribution gives the following expression:

$$\int \frac{\partial f}{\partial t}\,\partial v = -\frac{\varepsilon}{(K-\hat{K})}\int \left(f - (\tfrac{4}{3}\pi\hat{K})^{-3/2} e^{3v_n'v_n'/4K}\right)\partial v. \tag{A1}$$

Since both distributions integrate to 1, we can see that

$$\frac{\partial}{\partial t}\int f\,\partial v = 0. \tag{A2}$$

Conservation of momentum requires that no mean flow be created by the relaxation process. The mean velocity of the flow is equivalent to the first moment of the PDF. By taking the integral over all velocity space, we can show that

$$\int v_i \frac{\partial f}{\partial t}\,\partial v = -\frac{\varepsilon}{(K-\hat{K})}\int v_i\left(f - (\tfrac{4}{3}\pi\hat{K})^{-3/2} e^{3v_n'v_n'/4K}\right)\partial v. \tag{A3}$$

Using the fact that the velocity is an independent variable (from time) and splitting the velocity into its mean and fluctuating parts gives

$$\begin{aligned}\frac{\partial}{\partial t}\int v_i f\,\partial v &= -\frac{\varepsilon}{(K-\hat{K})}\left\{\int v_i f\,\partial v - u_i\int (\tfrac{4}{3}\pi\hat{K})^{-3/2} e^{3v_n'v_n'/4K}\,\partial v\right.\\ &\quad\left. - \int v_i'(\tfrac{4}{3}\pi\hat{K})^{-3/2} e^{3v_n'v_n'/4K}\,\partial v\right\}.\end{aligned} \tag{A4}$$

By definition $\int v_i f\,\partial v = u_i$. The second integral on the right-hand side is equal to 1 and the last integral is zero since it has an odd integrand, so finally

$$\frac{\partial}{\partial t}u_i = -\frac{\varepsilon}{(K-\hat{K})}\{u_i - u_i - 0\} = 0. \tag{A5}$$

The Reynolds transport equation is obtained by multiplying the PDF relation equation by $v_i'v_j'$ and then integrating over all velocity space,

$$\begin{aligned}&\int v_i'v_j'\frac{\partial f}{\partial t}\,\partial v\\ &= \frac{\partial R_{ij}}{\partial t} = -\frac{\varepsilon}{(K-\hat{K})}\int v_i'v_j'\left(f - (\tfrac{4}{3}\pi\hat{K})^{-3/2} e^{3v_n'v_n'/4K}\right)\partial v.\end{aligned} \tag{A6}$$

This then becomes

$$\begin{aligned}\frac{\partial}{\partial t}\int v_i'v_j' f\,\partial v &= -\frac{\varepsilon}{(K-\hat{K})}\left\{\int v_i'v_j' f\,\partial v\right.\\ &\quad\left. - (\tfrac{4}{3}\pi\hat{K})^{-3/2}\int v_i'v_j' e^{\frac{3v_n'v_n'}{4K}}\,\partial v\right\}.\end{aligned} \tag{A7}$$

Since $\int v_i'v_j' f\,\partial v = R_{ij}$ by definition, and the last integral must be isotropic

$$\frac{\partial R_{ij}}{\partial t} = -\frac{\varepsilon}{(K-\hat{K})}\{R_{ij} - \tfrac{2}{3}\hat{K}\delta_{ij}\}. \tag{A8}$$

APPENDIX B: RELAXATION MODEL MOMENTS

Here we verify conservation of mass for the relaxation models derived in Sec. IV. The method is the same as before starting from the relaxation model for the PDF,

$$\begin{aligned}\int \frac{\partial f}{\partial t}\,\partial v = \int C_M&\left(\frac{3\varepsilon}{2K}(\tfrac{4}{3}\pi\hat{K})^{-3/2} e^{-3\hat{v}_n'\hat{v}_n'/4\hat{K}}\right.\\ &\left. - \frac{3\varepsilon}{2K}\frac{\tilde{v}_n'\tilde{v}_n'}{2K + (u-\tilde{u})^2} f\right)\partial v\end{aligned} \tag{B1}$$

with $\hat{v}_i' = v_i - \hat{u}_i$, $\tilde{v}_i' = v_i - \tilde{u}_i$,

$$\int \frac{\partial f}{\partial t}\,\partial v = C_M\frac{3\varepsilon}{2K} - C_M\frac{3\varepsilon}{2K} \times\int \frac{(v_n' + u_n - \tilde{u}_n)(v_n' + u_n - \tilde{u}_n)}{2K + (u-\tilde{u})^2} f\,\partial v = 0. \tag{B2}$$

Since $\int v_n' f\,\partial v = 0$ we get

$$\int \frac{\partial f}{\partial t}\,\partial v = C_M\frac{3\varepsilon}{2K} - C_M\frac{3\varepsilon}{2K}\frac{1}{2K + (u-\tilde{u})^2} \times\int \left[(u_n - \tilde{u}_n)(u_n - \tilde{u}_n) + v_n'v_n'\right] f\,\partial v = 0. \tag{B3}$$

The integrals can be evaluated to give

$$\int \frac{\partial f}{\partial t}\,\partial v = C_M\frac{3\varepsilon}{2K} - C_M\frac{3\varepsilon}{2K}\frac{(u-\tilde{u})^2}{2K + (u-\tilde{u})^2} - C_M\frac{3\varepsilon}{2K}\frac{2K}{2K + (u-\tilde{u})^2} = 0. \tag{B4}$$

Similarly, to verify conservation of momentum we continue as follows:

$$\int v_i\frac{\partial f}{\partial t}\,\partial v = \frac{\partial u_i}{\partial t} = \int C_M v_i\left(\frac{3\varepsilon}{2K}\left(\tfrac{4}{3}\pi\hat{K}\right)^{-3/2} e^{-3\hat{v}_n'\hat{v}_n'/4\hat{K}} - \frac{3\varepsilon}{2K}\frac{\tilde{v}_n'\tilde{v}_n'}{2K + (u-\tilde{u})^2} f\right)\partial v \tag{B5}$$

expanding $v_n' = (u_n - \tilde{u}_n) + v_n'$ and $v_i = u_i + v_i'$ gives

$$\frac{\partial u_i}{\partial t} = C_M\frac{3\varepsilon}{2K}\hat{u}_i - C_M\frac{3\varepsilon}{2K}\frac{1}{2K + (u-\tilde{u})^2}\left((u-\tilde{u})^2 u_i + 2(u_n - \tilde{u}_n)R_{in} + 2Ku_i + \int v_i'v_n'v_n' f\,\partial v\right). \tag{B6}$$

Conservation requires the above equation be equal to zero, this implies that

$$\left[2K + (u-\tilde{u})^2\right](\hat{u}_i - u_i) = 2R_{in}(u_n - \tilde{u}_n) + \int v_i'v_n'v_n' f\,\partial v. \tag{B7}$$

From Appendix C, we see that if f is Gaussian, the last term on the right-hand side goes to zero, and $u_i = \tilde{u}_i = \hat{u}_i$ confirming conservation of momentum for Gaussian PDFs. For non-Gaussian PDFs the above relation must be satisfied.

The Reynolds stress transport equation is also derived similarly

$$\int v_i'v_j'\frac{\partial f}{\partial t}\,\partial v = \frac{\partial R_{ij}}{\partial t} = \int C_M v_i'v_j'\left(\frac{3\varepsilon}{2K}\left(\tfrac{4}{3}\pi\hat{K}\right)^{-3/2} e^{-3\hat{v}_n'\hat{v}_n'/4\hat{K}} - \frac{3\varepsilon}{2K}\frac{\tilde{v}_n'\tilde{v}_n'}{2K + (u-\tilde{u})^2} f\right)\partial v. \tag{B8}$$

By substituting in the relations $\hat{v}_i' = v_i - \hat{u}_i$ and $\tilde{v}_i' = v_i - \tilde{u}_i$ the integrals can be reduced,

$$\frac{\partial R_{ij}}{\partial t} = C_M\frac{3\varepsilon}{2K}\int [\hat{v}_i' + (\hat{u}_i - u_i)][\hat{v}_j' + (\hat{u}_j - u_j)] \times\left(\tfrac{4}{3}\pi\hat{K}\right)^{-3/2} e^{-3\hat{v}_n'\hat{v}_n'/4\hat{K}}\,\partial v - C_M\frac{3\varepsilon}{2K}\frac{1}{2K + (u-\tilde{u})^2} \times\int v_i'v_j'\big((u_n - \tilde{u}_n)(u_n - \tilde{u}_n) + 2v_n'(u_n - \tilde{u}_n) + v_n'v_n'\big) f\,\partial v. \tag{B9}$$

Since $\int \hat{v}_i'\left(\tfrac{4}{3}\pi\hat{K}\right)^{-3/2} e^{-3\hat{v}_n'\hat{v}_n'/4\hat{K}}\partial v = 0$ (due to the odd integrand), we get

$$\frac{\partial R_{ij}}{\partial t} = C_M\frac{3\varepsilon}{2K}\int [\hat{v}_i'\hat{v}_j' + (\hat{u}_i - u_i)(\hat{u}_j - u_j)] \times\left(\tfrac{4}{3}\pi\hat{K}\right)^{-3/2} e^{-3\hat{v}_n'\hat{v}_n'/4\hat{K}}\,\partial v - C_M\frac{3\varepsilon}{2K}\frac{1}{2K + (u-\tilde{u})^2} \times\left((u-\tilde{u})^2 R_{ij} + 2(u_n - \tilde{u}_n)\int v_i'v_j'v_n' f\,\partial v + \int v_i'v_f'v_n'v_n' f\,\partial v\right). \tag{B10}$$

The first integral is reduced in terms of "hats,"

$$\frac{\partial R_{ij}}{\partial t} = C_M\frac{3\varepsilon}{2K}\left[\tfrac{2}{3}\hat{K}\delta_{ij} + (\hat{u}_i - u_i)(\hat{u}_j - u_j)\right] - C_M\frac{3\varepsilon}{2K}\frac{1}{2K + (u-\tilde{u})^2}\left((u-\tilde{u})^2 R_{ij} + 2(u_n - \tilde{u}_n)\int v_i'v_j'v_n' f\,\partial v + \int v_i'v_j'v_n'v_n' f\,\partial v\right). \tag{B11}$$

To ensure the correct dissipation of energy, we require that the model satisfies the equation $\partial K/\partial t = \frac{1}{2}\partial R_{ii}/\partial t = -\varepsilon$,

$$-\frac{1}{2}\frac{\partial R_{ii}}{\partial t} = \varepsilon = -C_M\frac{3\varepsilon}{2K}\left[\hat{K} + \tfrac{1}{2}(\hat{u} - u)^2\right] + C_M\frac{3\epsilon}{2K}\frac{1}{2K + (u-\tilde{u})^2}\left((u-\tilde{u})^2 K + (u_n - \tilde{u}_n) \times\int v_i'v_j'v_n' f\,\partial v + \frac{1}{2}\int v_i'v_j'v_n'v_n' f\,\partial v\right). \tag{B12}$$

This can be simplified to

$$\hat{K}+\frac{1}{2}(\hat{u}-u)^2+\frac{2K}{3C_M} = \frac{1}{2K+(u-\tilde{u})^2}\Bigg((u-\tilde{u})^2K+(u_n-\tilde{u}_n) \times\int v_i'v_i'v_n'f\,\partial v+\frac{1}{2}\int v_i'v_i'v_n'v_n'f\,\partial v\Bigg) \tag{B13}$$

or finally

$$\left(\frac{\hat{K}}{K}+\frac{1}{2K}(\hat{u}-u)^2+\frac{2}{3C_M}\right)\left(2K+(u-\tilde{u})^2\right) = (u-\tilde{u})^2+\frac{u_n-\tilde{u}_n}{K}\int v_i'v_i'v_n'f\,\partial v + \frac{1}{2K}\int v_i'v_i'v_n'v_n'f\,\partial v. \tag{B14}$$

For an elliptic Gaussian PDF the above equation reduces to

$$\frac{\hat{K}}{K}+\frac{2}{3C_M}=\frac{1}{4K^2}\int v_i'v_i'v_n'v_n'f\,\partial v=\frac{1}{4K^2}\left(R_{nn}R_{ii}+2R_{ni}R_{ni}\right) \tag{B15}$$

or alternatively

$$\frac{\hat{K}}{K}=1-\frac{2}{3C_M}+\frac{R_{ni}R_{ni}}{2K^2}. \tag{B16}$$

This can be rearranged to become

$$\frac{3}{2}C_M=\left(1-\frac{\hat{K}}{K}+\frac{R_{ni}R_{ni}}{2K^2}\right)^{-1}. \tag{B17}$$

So if we assume Gaussian form for the PDF, the Reynolds transport equation can be written as follows:

$$\frac{\partial R_{ij}}{\partial t}=\frac{\varepsilon}{K}\left(1-\frac{\hat{K}}{K}+\frac{R_{ni}R_{ni}}{2K^2}\right)^{-1}\left(\frac{2}{3}\hat{K}\delta_{ij}\right) - \frac{\varepsilon}{K}\left(1-\frac{\hat{K}}{K}+\frac{R_{ni}R_{ni}}{2K^2}\right)^{-1}\frac{1}{2K}(R_{nn}R_{ij}+2R_{ni}R_{nj}). \tag{B18}$$

This simplifies to

$$\frac{\partial R_{ij}}{\partial t}=\frac{\varepsilon}{K}\frac{1}{1-\frac{\hat{K}}{K}+\frac{R_{mn}R_{mn}}{2K^2}}\left(\tfrac{2}{3}\hat{K}\delta_{ij}-R_{ij}-\frac{R_{ni}R_{nj}}{K}\right). \tag{B19}$$

Rearranging into the classic return model form gives

$$\frac{\partial R_{ij}}{\partial t}=-\frac{\varepsilon}{K}R_{ij}-\frac{\varepsilon}{K}\frac{\frac{\hat{K}}{K}-\frac{R_{mn}R_{mn}}{2K^2}}{1-\frac{\hat{K}}{K}+\frac{R_{mn}R_{mn}}{2K^2}}\left(R_{ij}-\tfrac{2}{3}K\delta_{ij}\right) + \frac{\varepsilon}{K^2}\frac{1}{1-\frac{\hat{K}}{K}+\frac{R_{mn}R_{mn}}{2K^2}}R_{mn}R_{mn}\frac{\delta_{ij}}{3} - \frac{\varepsilon}{K^2}\frac{1}{1-\frac{\hat{K}}{K}+\frac{R_{ni}R_{ni}}{2K^2}}R_{ni}R_{nj}. \tag{B20}$$

And when written as follows, the values of C_R and C_N become apparent:

$$\frac{\partial R_{ij}}{\partial t}=-\frac{\varepsilon}{K}R_{ij}-\frac{\varepsilon}{K}\left(\frac{\frac{4}{3}+\frac{\hat{K}}{K}-\frac{R_{ni}R_{ni}}{2K^2}}{1-\frac{\hat{K}}{K}+\frac{R_{ni}R_{ni}}{2K^2}}+\frac{4}{3}\frac{-1}{1-\frac{\hat{K}}{K}+\frac{R_{ni}R_{ni}}{2K^2}}\right) \times\left(R_{ij}-\frac{2}{3}K\delta_{ij}\right)+\frac{\varepsilon}{K^2}\frac{-1}{1-\frac{\hat{K}}{K}+\frac{R_{ni}R_{ni}}{2K^2}}\Bigg(R_{ni}R_{nj} - R_{ni}R_{ni}\frac{\delta_{ij}}{3}\Bigg). \tag{B21}$$

APPENDIX C: MOMENTS OF A GAUSSIAN PROBABILITY DENSITY FUNCTION

If we have a PDF of elliptic Gaussian shape we can write the PDF as

$$f=\left[(2\pi)^3\det(R_{nm})\right]^{-1/2}e^{(1/2)R_{nm}^{-1}v_n'v_m'}. \tag{C1}$$

Since only R_{ij} is a function of space, this implies that the derivative satisfies

$$-R_{kl}\frac{\partial f}{\partial v_k}=v_l'f. \tag{C2}$$

This allows us to write the third moment as a second moment and then apply the chain rule,

$$\int v_i'v_n'v_m'f\,\partial v=-R_{km}\int v_i'v_n'\frac{\partial f}{\partial v_k}\,\partial v = -R_{km}\int\left(\frac{\partial v_i'v_n'f}{\partial v_k}-f\frac{\partial v_i'v_n'}{\partial v_k}\right)\partial v. \tag{C3}$$

By Gauss's divergence theorem the first integral term goes to zero, since $f\to 0$ at infinity. Differentiating the second term gives

$$\int v_i' v_n' v_m' f\,\partial v = R_{km}\int f\left(v_i'\delta_{nk} + v_n'\delta_{ik}\right)\partial v$$
$$= R_{nm}\int v_i' f\,\partial v + R_{im}\int v_n' f\,\partial v = 0, \quad \text{(C4)}$$

which is what we would expect since the PDF is an even function and the integrand is an odd function (cubic).

The expression (A2) and the chain rule is also useful for evaluating the fourth moment of an elliptic Gaussian,

$$\int v_m' v_n' v_i' v_j' f d\mathbf{v} = -R_{kj}\int v_m' v_n' v_i' \frac{\partial f}{\partial v_k} d\mathbf{v}$$
$$= R_{kj}\int f \frac{\partial v_m' v_n' v_i'}{\partial v_k} d\mathbf{v}. \quad \text{(C5)}$$

Taking the derivative gives the fourth moment in terms of the second moments

$$= R_{kj}\int f\left(v_m' v_n' \delta_{ik} + v_n' v_i' \delta_{mk} + v_m' v_i' \delta_{nk}\right) d\mathbf{v}$$
$$= R_{mn}R_{ij} + R_{ni}R_{mj} + R_{mi}R_{nj}. \quad \text{(C6)}$$

APPENDIX D: GENERAL RELAXATION MOMENTS

Here we verify conservation of mass for the more general relaxation models derived in Sec. VI. The method is the same as before starting from the general relaxation model for the PDF, Eq. (33). Conservation of mass then requires that the right-hand side of the zeroth moment be equal to zero,

$$\int \frac{\partial f}{\partial t}\partial v = C_M \frac{\varepsilon}{2K}\int \Pi_{ii}[(2\pi)^3 \det(\hat{R}_{nm})]^{-1/2}$$
$$\times e^{-(1/2)\hat{R}_{nm}^{-1}\hat{v}_n'\hat{v}_m'}\partial v - C_M\frac{\varepsilon}{2K}$$
$$\times \int \frac{\Pi_{in}R_{im}^{-1}\tilde{v}_m'\tilde{v}_n'}{1 + (u_n - \tilde{u}_n)(u_m - \tilde{u}_m)\dfrac{\Pi_{in}}{\Pi_{pp}}R_{im}^{-1}} f\,\partial v, \quad \text{(D1)}$$

$$\int \frac{\partial f}{\partial t}\partial v = C_M\frac{\varepsilon}{2K}\Pi_{ii} - C_M\frac{\varepsilon}{2K}$$
$$\times \frac{\Pi_{in}R_{im}^{-1}}{1 + (u_n - \tilde{u}_n)(u_m - \tilde{u}_m)\dfrac{\Pi_{in}}{\Pi_{pp}}R_{im}^{-1}}$$
$$\times \int \tilde{v}_m'\tilde{v}_n' f\,\partial v. \quad \text{(D2)}$$

Substituting with $\tilde{v}_i' = v_i' + u_i - \tilde{u}_i$, and recalling that $\int v_m' f\,\partial v = 0$ gives

$$\int \frac{\partial f}{\partial t}\partial v = C_M\frac{\varepsilon}{2K}\Pi_{ii} - C_M\frac{\varepsilon}{2K}$$
$$\times \frac{\Pi_{in}R_{im}^{-1}}{1 + (u_n - \tilde{u}_n)(u_m - \tilde{u}_m)\dfrac{\Pi_{in}}{\Pi_{pp}}R_{im}^{-1}}$$
$$\times \int [v_m' v_n' + (u_m - \tilde{u}_m)(u_n - \tilde{u}_n)] f\,\partial v, \quad \text{(D3)}$$

$$\int \frac{\partial f}{\partial t}\partial v = C_M\frac{\varepsilon}{2K}\Pi_{ii} - C_M\frac{\varepsilon}{2K}$$
$$\times \frac{\Pi_{in}R_{im}^{-1}}{1 + (u_n - \tilde{u}_n)(u_m - \tilde{u}_m)\dfrac{\Pi_{in}}{\Pi_{pp}}R_{im}^{-1}}$$
$$\times [R_{mn} + (u_m - \tilde{u}_m)(u_n - \tilde{u}_n)] = 0. \quad \text{(D4)}$$

The momentum equation is the first moment

$$\frac{\partial u_p}{\partial t} = C_M\frac{\varepsilon}{2K}\prod_{ii}\int v_p[(2\pi)^3\det(\hat{R}_{nm})]^{-1/2}e^{-(1/2)\hat{R}_{nm}^{-1}\hat{v}_n'\hat{v}_m'}\partial v$$
$$- C_M\frac{\varepsilon}{2K}\int \frac{\Pi_{in}R_{im}^{-1}\tilde{v}_m'\tilde{v}_n'}{1 + (u_n - \tilde{u}_n)(u_m - \tilde{u}_m)\dfrac{\Pi_{in}}{\Pi_{pp}}R_{im}^{-1}} v_p f\,\partial v, \quad \text{(D5)}$$

$$\frac{\partial u_p}{\partial t} = C_M\frac{\varepsilon}{2K}\Pi_{ii}\hat{u}_p$$
$$- C_M\frac{\varepsilon}{2K}\frac{\Pi_{in}R_{im}^{-1}}{1 + (u_n - \tilde{u}_n)(u_m - \tilde{u}_m)\dfrac{\Pi_{in}}{\Pi_{pp}}R_{im}^{-1}}$$
$$\times \int [v_m' + (u_m - \tilde{u}_m)][v_n' + (u_n - \tilde{u}_n)] v_p f\,\partial v, \quad \text{(D6)}$$

$$\frac{\partial u_p}{\partial t} = C_M\frac{\varepsilon}{2K}\Pi_{ii}\hat{u}_p$$
$$- C_M\frac{\varepsilon}{2K}\frac{\Pi_{in}R_{im}^{-1}}{1 + (u_n - \tilde{u}_n)(u_m - \tilde{u}_m)\dfrac{\Pi_{in}}{\Pi_{pp}}R_{im}^{-1}}$$
$$\times \left(\int v_m' v_n' v_p' f\,\partial v + R_{mn}u_p\right)$$
$$- C_M\frac{\varepsilon}{2K}\frac{\Pi_{in}R_{im}^{-1}}{1 + (u_n - \tilde{u}_n)(u_m - \tilde{u}_m)\dfrac{\Pi_{in}}{\Pi_{pp}}R_{im}^{-1}}$$
$$\times [R_{mp}(u_n - \tilde{u}_n) + R_{np}(u_m - \tilde{u}_m)$$
$$+ (u_m - \tilde{u}_m)(u_n - \tilde{u}_n)u_p]. \quad \text{(D7)}$$

Conservation of momentum therefore requires that

$$C_M\frac{\varepsilon}{2K}\Pi_{ii}\hat{u}_p = C_M\frac{\varepsilon}{2K}\frac{\Pi_{in}R_{im}^{-1}}{1+(u_n-\tilde{u}_n)(u_m-\tilde{u}_m)\frac{\Pi_{in}}{\Pi_{pp}}R_{im}^{-1}} \times\left\{\int v_m'v_n'v_p'f\,\partial v + R_{mn}u_p + [R_{mp}(u_n-\tilde{u}_n) + R_{np}(u_m-\tilde{u}_m) + (u_m-\tilde{u}_m)(u_n-\tilde{u}_n)u_p]\right\}, \tag{D8}$$

which simplifies to

$$\hat{u}_p\left[1+(u_n-\tilde{u}_n)(u_m-\tilde{u}_m)\frac{\Pi_{in}}{\Pi_{pp}}R_{im}^{-1}\right] = \frac{\Pi_{in}R_{im}^{-1}}{\Pi_{ii}}\int v_m'v_n'v_p'f\,\partial v + u_p + \frac{\Pi_{in}}{\Pi_{ii}}R_{im}^{-1}[R_{mp}(u_n-\tilde{u}_n) + R_{np}(u_m-\tilde{u}_m)] + \frac{\Pi_{in}}{\Pi_{ii}}R_{im}^{-1}(u_m-\tilde{u}_m)(u_n-\tilde{u}_n)u_p \tag{D9}$$

and

$$(\hat{u}_p-u_p)\left[1+(u_n-\tilde{u}_n)(u_m-\tilde{u}_m)\frac{\Pi_{in}}{\Pi_{pp}}R_{im}^{-1}\right] = \frac{\Pi_{in}}{\Pi_{ii}}R_{im}^{-1}\left(\int v_m'v_n'v_p'f\,\partial v + R_{mp}(u_n-\tilde{u}_n) + R_{np}(u_m-\tilde{u}_m)\right). \tag{D10}$$

APPENDIX E: GENERAL REYNOLDS TRANSPORT EQUATION

Below, the Reynolds transport equation is derived for the general relaxation model,

$$\frac{\partial R_{lp}}{\partial t} = C_M\frac{\varepsilon}{2K}\left(\Pi_{ii}\int v_l'v_p'[(2\pi)^3\det(\hat{R}_{nm})]^{-1/2} \times e^{-(1/2)\hat{R}_{nm}^{-1}\hat{v}_n'\hat{v}_m'}\,\partial v - \int\frac{\Pi_{in}R_{im}^{-1}\tilde{v}_m'\tilde{v}_n'}{1+(u_n-\tilde{u}_n)(u_m-\tilde{u}_m)\frac{\Pi_{in}}{\Pi_{pp}}R_{im}^{-1}}v_l'v_p'f\,\partial v\right). \tag{E1}$$

Substitution gives

$$\frac{\partial R_{lj}}{\partial t} = C_M\frac{\varepsilon}{2\hat{K}}\Pi_{ii}\int[\hat{v}_l'\hat{v}_j' + (\hat{u}_l-u_l)(\hat{u}_j-u_j)] \times[(2\pi)^3\det(\hat{R}_{nm})]^{-1/2}e^{-(1/2)\hat{R}_{nm}^{-1}\hat{v}_n'\hat{v}_m'}\,\partial v - C_M\frac{\varepsilon}{2\hat{K}}\frac{\Pi_{in}R_{im}^{-1}}{1+(u_n-\tilde{u}_n)(u_m-\tilde{u}_m)\frac{\Pi_{in}}{\Pi_{pp}}R_{im}^{-1}} \times\int v_l'v_j'\tilde{v}_m'\tilde{v}_n'f\,\partial v, \tag{E2}$$

$$\frac{\partial R_{lj}}{\partial t} = C_M\frac{\varepsilon}{2\hat{K}}\left(\Pi_{ii}\hat{R}_{lj} + \Pi_{ii}(\hat{u}_l-u_l)(\hat{u}_j-u_j) - \frac{\Pi_{in}R_{im}^{-1}}{1+(u_n-\tilde{u}_n)(u_m-\tilde{u}_m)\frac{\Pi_{in}}{\Pi_{pp}}R_{im}^{-1}}\int v_l'v_j'\tilde{v}_m'\tilde{v}_n'f\,\partial v\right). \tag{E3}$$

If we choose $u_n=\tilde{u}_n$ and use the general form of the Reynolds stress model, $\partial R_{lj}/\partial t=-(\varepsilon/2K)(\Pi_{im}R_{mj}+\Pi_{jm}R_{mi})$, we arrive at the following equation:

$$-(\Pi_{im}R_{mj}+\Pi_{jm}R_{mi}) = C_M\Pi_{ii}\left(\hat{R}_{lj} + (\hat{u}_l-u_l)(\hat{u}_j-u_j) - \frac{\Pi_{in}R_{im}^{-1}}{\Pi_{ii}}\int v_l'v_j'v_m'v_n'f\,\partial v\right), \tag{E4}$$

which gives us the definition of $\hat{R}$

$$\hat{R}_{lj} = \frac{-1}{C_M\Pi_{ii}}(\Pi_{im}R_{mj}+\Pi_{jm}R_{mi}) - (\hat{u}_l-u_l)(\hat{u}_j-u_j) + \frac{\Pi_{in}R_{im}^{-1}}{\Pi_{ii}}\int v_l'v_j'v_m'v_n'f\,\partial v. \tag{E5}$$

[1]J. Rotta, "Stastische theorie nichthomegener turbulenz I," Z. Phys. **129**, 547 (1951).

[2]J. L. Lumley, "Computation modeling of turbulent flows," Adv. Appl. Mech. **18**, 126 (1978).

[3]L. Le Penven, J. N. Gence, and G. Comte-Bellot, "On the approach to isotropy of homogeneous turbulence: Effect of the partiton of kinetic energy among the velocity components," in *Frontiers in Fluid Mechanics*, edited by S. H. Davis and J. L. Lumley (Springer, New York, 1985), p. 1.

[4]S. Sarkar and C. G. Speziale, "A simple nonlinear model for the return to isotropy in turbulence," Phys. Fluids A **2**, 84 (1990).

[5]D. C. Haworth and S. B. Pope, "A generalized Langevin model for turbulent flows," Phys. Fluids **29**, 2 (1986).

[6]K. S. Choi and J. L. Lumley, "Turbulence and chaotic phenomena in fluids," in *Proceedings of the IUTAM Symposium (Kyoto, Japan)*, edited by T. Tatsumi (North-Holland, Amsterdam, 1984), p. 267.

[7]K. S. Choi and J. L. Lumley, "The return to isotropy of homogeneous turbulence," J. Fluid Mech. **436**, 57 (2001).

[8]T. J. Craft and B. E. Launder, "Computation of impinging flows using second-moment closure," in *Proceedings of the Eighth Symposium on Turbulent Shear Flows* (Technical University of Munich, Munich, Germany, 1991), pp. 8-5-1–8-5-6.

[9]M. Yamamoto and C. Arakawa, "Study on the pressure-strain term in Reynolds stress models," in *Proceedings of the Eighth Symposium on Turbulent Shear Flows* (Technical University of Munich, Munich, Germany, 1991), pp. III-17-1–III-17-2.

[10]C. G. Speziale, S. Sarkar, and T. B. Gatski, "Modeling the pressure-strain correlation of turbulence: An invariant dynamical systems approach," J. Fluid Mech. **227**, 245 (1991).

[11]P. Degond and M. Lemou, in *Hyperbolic Problems, Theory, Numerics and Applications Eighth International Conference in Magdeburg, February–March 2000*, edited by H. Freistueler and G. Warnecke (Birkhauser, Boston, 2001).

[12]P. Bhatnagar, E. P. Gross, and M. K. Krook, "A model of collision processes in gases. I. Small amplitude processes in charged and neutral one-component systems," Phys. Rev. **94**, 511 (1954).

[13]M. Hallbäck, J. Groth, and A. V. Johansson, "An algebraic model for nonisotropic turbulent dissipation rate in Reynolds stress closures," Phys. Fluids A **2**, 1859 (1990).

[14]J. B. Perot and P. Moin, "A near wall model for the dissipation tensor,"

Eleventh Australasian Fluid Mechanics Conference, Hobart, Tasmania, Australia, 13-18, 1992.
[15] P. A. Durbin and B. A. Pettersson Reif, *Statistical Theory and Modeling for Turbulent Flows* (Wiley, New York, 2001).
[16] B. E. Launder, G. J. Reece, and W. Rodi, "Progress in the development of a Reynolds stress turbulence closure," J. Fluid Mech. **68**, 537 (1975).
[17] T. Sjögren and A. V. Johansson, "Development and calibration of algebraic nonlinear models for terms in the Reynolds stress transport equation," Phys. Fluids **12**, 1554 (2000).
[18] U. Schumann, "Realizability of Reynolds stress turbulence models," Phys. Fluids **20**, 721 (1977).
[19] S. B. Pope, *Turbulent Flows* (Cambridge University Press, Cambridge, 2000).
[20] S. Tavoularis and S. Corrsin, "Experiments in nearly homogeneous turbulent shear flow with a uniform mean temperature gradient. Part 1," J. Fluid Mech. **104**, 311 (1981).
[21] P. K. Yeung and S. B. Pope, "Lagrangian statistics from direct numerical simulations of isotropic turbulence," J. Fluid Mech. **207**, 531 (1989).
[22] P. G. Saffman, "Note on decay of homogeneous turbulence," Phys. Fluids **10**, 1349 (1967).
[23] J. P. Laval, B. Dubrulle, and J. C. McWilliams, "Langevin models of turbulence: Renormalization group, distant interaction algorithms, or rapid distortion theory?" Phys. Fluids **15**, 5 (2003).
[24] C. Chartrand, "Eddy collision models for turbulence," Masters thesis, University of Massachusetts, Amherst, 2003.